Limits and special symmetries of extremal black holes

Helgi Freyr Rúnarsson

Master thesis in Theoretical Physics

Department of Physics

Stockholm University

Stockholm, Sweden 2012

Abstract

Limits of spacetimes are obtained through a coordinate dependent procedure and in particular, limits of black hole spacetimes yield limit spacetimes that are some variants of anti-de Sitter space. These limits are of use in string theory, and in particular in the adS/CFT correspondence. By defining null coordinates, we are able to derive these limits in a clearer fashion for the whole spacetime and analyzing these new coordinates and the limit spacetimes, we see which region of the limit spacetime is covered by these coordinates.

Conformal isometries are special symmetries of spacetimes where the light cone structure of the spacetime is conserved. The charged black hole in a cosmological background possesses a discrete conformal isometry for certain values of its parameters and we show that this conformal isometry extends throughout the whole spacetime and beyond.

The Killing vector fields of the spinning black hole give insight into how an observer can move in certain regions of the spacetime. In particular, the so called velocity of light surface tells us where an observer can no longer corotate with the black hole. For an extremal black hole, we find that this surface lies both inside and outside the horizon of the black hole.

Acknowledgements

I would like to thank my supervisor Ingemar Bengtsson for being a source of inspiration, guiding me along the correct paths to take and clearing up misconceptions of concepts during proofreading of the thesis. I would also like to thank him for suggesting the topic in the first place, as I am very satisfied with the way it went and finally got a chance to delve deep into topics I had always had an interest in looking at.

I would also like to thank Jan Åman for various symbolic calculations through out the work of this thesis.

I would also like to thank Kristín for being the wall I could bounce my ideas off. It has been extremely helpful to be able to get feedback and confirmation or rejection of my thoughts during this process.

Contents

Chapter 1

Introduction

In *physical* terms, a black hole is a region of spacetime from which nothing can escape, light ray or otherwise. In more *mathematical* terms, a black hole is the complement of the chronological past of future null infinity of an asymptotically flat spacetime or

$$\mathscr{B} = M - J^{-}\left(\mathscr{I}^{+}\right), \tag{1.1}$$

where M is the spacetime, J^{-} is the causal past and $\mathscr{I}^{+}$ is future null infinity. These terms require some explanation.

The *causal past* of a point p in a spacetime M is defined as the set of events that can be reached by a past directed causal curve starting from p. The *causal future* of a point p is defined analogously but we will not need that in this thesis. The causal past of a surface S as it is used in the equation above, is simply the union of the causal pasts of all points in S. In simple terms, *future null infinity*, $\mathscr{I}^{+}$, is the surface where future directed null curves end. Likewise, *past null infinity*, $\mathscr{I}^{-}$, is the surface where past directed null curves end. We will see an example of these surfaces later in this thesis. An *asymptotically flat* spacetime has the property that at infinity the metric that describes the spacetime approaches the metric of flat space in appropriate coordinates. Another way to define an asymptotically flat spacetime is to say that one can attach the hypersurfaces $\mathscr{I}^{\pm}$ to it. With these definitions at hand we see that these first two definitions of black holes describe the same property but in two different languages.

The *event horizon*, H, of the black hole is the boundary of $\mathscr{B}$,

$$H = \dot{J}^{-}\left(\mathscr{I}^{+}\right) \cap M, \tag{1.2}$$

where $\dot{J}^{-}$ is the boundary of J^{-}. That is, the event horizon is a region of no return and once an observer passes into it, he can not escape from the black hole.

	Non-rotating ($a = 0$)	Rotating ($a \neq 0$)
Uncharged ($e = 0$)	Schwarzschild	Kerr
Charged ($e \neq 0$)	Reissner-Nordström	Kerr-Newman

Table 1.1: The different types of stationary black holes.

In more *practical* terms, a black hole is a solution to second order, non-linear, partial differential equations for the metric tensor g_{ab}, the Einstein-Maxwell equations,

$$R_{ab} - \frac{1}{2} g_{ab} R + \lambda g_{ab} = 8\pi T_{ab}, \tag{1.3}$$

where R_{ab} is the Ricci tensor, R is the Ricci scalar, T_{ab} is the stress-energy tensor and λ is the cosmological constant. It turns out that the solutions we are interested in, force T_{ab} to take on a very special form due to the spacetimes being electrovac. The equation is written in the so-called geometric units, where the speed of light c, the gravitational constant G and Coulomb's constant k_e are all equal to one and are dimensionless. We will use these units in the rest of this thesis. Solutions to this equation that describe black hole spacetimes are electrovac and in the case of this thesis, stationary. That is, the spacetimes we will consider possess a timelike Killing vector field and the only matter fields they have will be electromagnetic fields.

Surprisingly, black holes are described by only three parameters once the cosmological constant has been fixed: Their mass m, charge e and angular momentum (per unit mass) $a = j/m$, where j is the angular momentum. These parameters are defined by the gravitational and electromagnetic fields far from the hole. Assuming that a black hole must have mass, we conclude that there are four types of black holes. These are depicted in table 1.1 and their names given.

One thing that all four types of black holes have in common is the existence of horizons, as we know from the second definition of a black hole above. While some of them have multiple horizons, it is always the case that the outermost horizon of the spacetime is the previously mentioned event horizon. As indicated in the definitions of black holes above, nothing escapes from the black hole once it is within the event horizon.

As we will see in chapters 5 and 6, the dimensionless ratio of the charge and the mass or angular momentum and the mass squared is of vital importance to the geometry of the black hole. It so happens that in the units used in equation (1.3) these ratios are dimensionless without the help of any constants as m, e and a all have the same units. That is, these ratios are simply e/m and $j/m^2 = a/m$. When this ratio is unity, the geometry changes dramatically and black holes with this property are

called extremal. The namesake comes from the fact that this value of the charge or angular momentum is the highest value where the spacetime has a horizon. We will see how this happens in practice in chapters 5 and 6, where the positions of the horizons are given in terms of m and a or e. As an example, the dimensionless charge to mass ratio for an electron is of the order of $e/m_e \approx 10^{21}$ and the dimensionless angular momentum to mass squared ratio for the Earth is $a_E/m_E \approx 894$ while for the sun it is $a_\odot/m_\odot \approx 1.25$. This implies that black holes are restricted to relatively low values of charge and angular momentum compared to other objects. If the Sun or Earth were to become black holes, they would have to shed a considerable amount of their rotational angular momentum in the process.

It has been argued in various ways that one cannot spin a black hole up beyond, or even up to, the extremal value. As Thorne points out[1], when one tries to spin up a black hole by infall of particles from the inner edge of an accretion disk, there is an upper limit on the achievable ratio of the angular momentum and the mass. This ratio is less than unity and is a indication that a black hole can not be spun up to extremality. On top of this, it turns out that black holes tend to have low electric charge. All hope is not lost since in string theory extremal black holes are of particular interest because in these extremal cases, it has been possible to calculate black hole entropy from first principles. Therefore the mathematical properties of such black holes are of importance.

The horizons of black holes have many interesting properties. In a large part of this thesis we will focus on investigating the geometry very close to the horizon of the black hole, in the so called near-horizon limit. There the metric takes on a certain form as we will see in chapters 5 and 6. In particular, in all the limits we will discuss it turns out that the limit spacetime involve some variants of anti de-Sitter space, which will be discussed in chapter 3.

Taking limits of spacetimes has to be done with care as it is a *coordinate dependent* procedure. This is most easily demonstrated by a simple example.

The Schwarzschild black hole is described by the metric

$$ds^2 = -\left(1 - \frac{2m}{r}\right) dt^2 + \frac{dr^2}{1 - \frac{2m}{r}} + r^2 d\Omega_2^2, \tag{1.4}$$

where $d\Omega_2$ is the metric of the two-sphere, $d\Omega_2^2 = d\theta^2 + \sin^2\theta d\phi^2$. A possible limit to investigate is letting the mass tend to infinity, but in this form of the metric, the limit is ill defined so we have to make a change of coordinates. The first set of coordinates we will use are defined by

$$x = r + m^{4/3}, \qquad \theta' = m^{4/3}\theta. \tag{1.5}$$

After performing this transformation and letting the mass go to infinity, the metric takes the form

$$ds^2 = -dt^2 + dx^2 + d\theta'^2 + \theta'^2 d\phi^2, \tag{1.6}$$

which is Minkowski space in cylindrical coordinates. However, if we instead use the coordinates defined by

$$r' = m^{-1/3} r, \qquad t' = m^{1/3} t, \qquad \theta' = m^{1/3}\theta, \tag{1.7}$$

and let $m \to \infty$, the metric becomes

$$ds^2 = \frac{2}{r'} dt'^2 - \frac{r'}{2} dr'^2 + r'^2 \left(d\theta'^2 + \theta'^2 d\phi^2 \right), \tag{1.8}$$

which is the so called Kasner metric, a non-flat solution to Einstein's equations and describes an anisotropic universe without matter[2]. We see that in this limit, two totally different *limit spacetimes* are obtained depending on the choice of coordinates. While the two limits we will look at in this thesis turn out to be the same limit obtained via different paths this is however a good reminder that one must take care when taking limits of spacetimes and be clear as to what coordinate system is being used.

Along with the limits of the charged and spinning black holes in chapters 5 and 6, respectively, we will look at conformal isometries of the charged black hole in a cosmological background and Killing vector fields of the spinning black hole. To prepare for this, we will discuss Killing vector fields and conformal spacetimes and isometries in chapter 2.

In chapter 4 we will discuss Carter-Penrose diagrams. These are conformally compactified diagrams of spherically symmetric spacetimes that capture the essential causal properties of the spacetime in a simple two dimensional diagram. These diagrams will be helpful when analyzing the Reissner-Nordström spacetime, both with and without a cosmological constant.

Chapter 2

Various mathematical topics

In this thesis we will be interested in many properties of the black hole spacetimes in question. This chapter will introduce the most important of these properties and explain them before looking at the black hole spacetimes themselves. First we will look at Killing vector fields and discuss what they tell us about the spacetime. After that we will see what it means for two spacetimes to be conformal and what it means if a spacetime has a conformal isometry.

It is assumed that the reader is familiar with general relativity at the level of an introductory course using, for example, Schutz's book[3].

2.1 Killing vector fields

A vector field ξ^a is a Killing vector field if the Lie derivative with respect to ξ^a of the metric vanishes, that is

$$\pounds_\xi g_{ab} = 0. \tag{2.1}$$

From the definition of a Lie derivative of a second rank tensor this gives Killing's equation

$$\begin{aligned} \pounds_\xi g_{ab} &= \xi^c \nabla_c g_{ab} + g_{cb}\nabla_a \xi^c + g_{ac}\nabla_b \xi^c \\ &= \nabla_a \xi_b + \nabla_b \xi_a, \end{aligned} \tag{2.2}$$

where the second equality sign holds when ∇_a is the derivative operator associated with g_{ab}. Notice from this that a linear combination of two vector fields that both satisfy equation (2.2) on their own, is also a Killing vector field. In physical terms, flows generated by Killing vector fields are continuous isometries of the manifold. More simply, the flow generates a symmetry in the sense that moving along it in the spacetime will not change the spacetime.

In terms of the metric, an easy way to find some Killing vector fields is simply to see which coordinates the metric is independent of. Let us use the Schwarzschild metric, defined by equation (1.4), as an example. We notice immediately that g_{ab} is independent of both t and ϕ which means that moving along a vector field that lies along these coordinates will not change the spacetime. That is ∂_t and ∂_ϕ are both Killing vector fields. These Killing vector fields correspond to time translational symmetry and rotational symmetry around the z axis, respectively. However, there are also two Killing vector fields that are not at all obvious from the form of the metric. These are

$$\sin\phi\partial_\theta + \cot\theta\cos\phi\partial_\phi, \qquad \cos\phi\partial_\theta - \cot\theta\sin\phi\partial_\phi, \tag{2.3}$$

which correspond to the two remaining rotational symmetries of the two-sphere. Along with ∂_ϕ these two Killing vectors generate the Lie group $SO(3)$.

In what follows, it will be important to know how a Killing vector field behaves under coordinate transformation. For simplicity let us assume that a spacetime has the Killing vector field $\xi^a = (\partial_t)^a$ where t is one of its coordinates. For both the charged and spinning black hole it is beneficial to perform a coordinate transform of the form

$$t \to \tilde{t} = t - f(r), \tag{2.4}$$

where r is another coordinate of the spacetime and $f(r)$ is some function of r. We know that a derivative transforms covariantly and therefore

$$\partial_{\tilde{t}} = \frac{\partial t}{\partial \tilde{t}}\partial_t - \frac{\partial f}{\partial \tilde{t}}\frac{\partial r}{\partial f}\partial_r, \tag{2.5}$$

but since r, and therefore $f(r)$, is independent of $\tilde{t}$ we see that this reduces to

$$\partial_{\tilde{t}} = \partial_t. \tag{2.6}$$

We will use this when we discuss the Killing vector fields of the spinning black hole spacetime in chapter 6.

2.1.1 Surface gravity for a spherically symmetric metric

As an example of what Killing vectors can be used for, we will derive the surface gravity of a spherically symmetric metric.

The surface gravity of an object is the gravitational acceleration experienced at its surface. As a familiar example, the surface gravity of the Earth is $g \approx 9.8m/s^2$. However, when dealing with black holes the acceleration of a test particle at the event horizon turns out to be infinite. Due to this, a renormalized value is used. This new value corresponds to the Newtonian value in the non-relativistic limit and is generally defined as the local proper acceleration multiplied by the gravitational redshift factor. The former diverges at the event horizon while the latter goes to zero.

If k^a is a Killing vector field which goes null on a particular hypersurface and the hypersurface is also null, we say that it is a Killing horizon. Note that for any null hypersurface, the normal vector is tangent to the hypersurface itself. This defines a vector field on the hypersurface and the flow lines are null geodesics. It follows that the Killing vector field goes along these geodesics.

From all of this, it follows that[4]

$$\nabla_a k^2 = 2\kappa k_a, \tag{2.7}$$

where we can choose $\kappa \geq 0$ by changing the sign of k as needed. κ is the surface gravity of a black hole whose event horizon is a Killing horizon, and we can rewrite equation (2.7) as

$$k^a \nabla_a k^b = \kappa k^b, \tag{2.8}$$

which is to be evaluated at the horizon.

We are interested in metrics of the form

$$ds^2 = -V(r)dt^2 + V^{-1}(r)dr^2 + r^2 d\Omega_2^2. \tag{2.9}$$

The metric has a timelike Killing vector

$$\chi = \partial_t, \tag{2.10}$$

which has a norm

$$\begin{aligned} \|\chi\|^2 &= g_{tt} \\ &= -V(r). \end{aligned} \tag{2.11}$$

To calculate the surface gravity, we use that equation (2.8) implies

$$\nabla_a \chi^b \chi_b = -2\kappa \chi_a, \tag{2.12}$$

where κ is the surface gravity. Combining these two equations yields

$$\nabla_a V(r) = 2\kappa g_{ab}\chi^b.$$

If we now, transform coordinates such that

$$t = t' - f(r'), \tag{2.13}$$
$$r = r', \tag{2.14}$$

We see that this transformation puts the metric into the form

$$ds^2 = -V(r')dt'^2 + 2V(r')f'(r')dt'dr' + \frac{dr'^2}{V(r')}\left(1 - V^2(r')f'^2(r')\right). \tag{2.15}$$

Choosing f' such that $1 - V^2 f'^2 = V$ and putting $a = r'$ we see that

$$\begin{aligned}\frac{\partial}{\partial r'}V(r') &= 2\kappa g_{r't'}\chi^{t'} \\ &= 2\kappa V(r')f'(r') \\ &= \pm 2\kappa\sqrt{1 - V(r')},\end{aligned}$$

or

$$\kappa = \frac{1}{2}\left|\frac{\frac{\partial}{\partial r}V(r)}{\sqrt{1 - V(r)}}\right|. \tag{2.16}$$

This was to be evaluated at the horizon and since $V(r) = 0$ at the horizon, we see that

$$\kappa = \frac{1}{2}\left|\frac{\partial}{\partial r}V(r)\right|_{r=r_0}, \tag{2.17}$$

where r_0 is a horizon, or in other words, a root of $V(r)$.

A few observations that will be useful for what is to come are in order.

- We see that κ has an absolute zero when the Killing horizon is degenerate. Note that this is the proper definition of an extremal black hole. That is, a black hole which has a degenerate Killing horizon.
- κ is only defined up to a constant factor that is fixed implicitly when the factor in front of the Killing vector is chosen.
- κ is constant along each generator and constant over the entire horizon[4].

These properties are similar to the properties of absolute temperature and if we look ahead, hint at that equation (5.20) makes sense.

2.2 Conformal spacetimes and isometries

Two spacetimes M and $\hat{M}$, described by the two metrics g and $\hat{g}$, are said to be conformal if

$$g = \Omega^2 \hat{g}. \tag{2.18}$$

This means that for any four vectors $\mathbf{x}$, $\mathbf{y}$, $\mathbf{v}$ and $\mathbf{w}$ at a point p the following holds

$$\frac{g\,(\mathbf{x},\mathbf{y})}{g\,(\mathbf{v},\mathbf{w})} = \frac{\hat{g}\,(\mathbf{x},\mathbf{y})}{\hat{g}\,(\mathbf{v},\mathbf{w})}, \tag{2.19}$$

where $g(\mathbf{x},\mathbf{y})$ is the inner product of $\mathbf{x}$ and $\mathbf{y}$ with respect to the metric g. This tells us that angles and ratios of magnitudes are conserved under a conformal transformation and that the null cone structure of the two spacetimes are the same. The geodesics of massive particles do however change but they only change in the direction of a coordinate that Ω is a function of. For example, a metric given by $g = \Omega(x)^2\eta$, where η is the metric of flat space, will have geodesics along the y and z directions as that of flat space while the geodesic along the x direction changes. A spacetime described by a metric with this property is said to be *conformally flat*.

It turns out that M could be a subset of $\hat{M}$. That is, $\hat{g}$ from equation (2.18) can be made to work in more than M. Including, and going beyond, $\mathscr{I}^{\pm}$. This means that the hypersurfaces $\mathscr{I}^{\pm}$, defined by $\Omega = 0$, are ordinary hypersurfaces in the unphysical spacetime $\hat{M}$. The spacetime $\hat{M}$ is therefore in a way unphysical as it goes beyond our physical spacetime M. Note that the word unphysical in this context is a technical term as the region of the spacetime $\hat{M}$ that is not in the spacetime M is unphysical with respect to M. In chapter 4 we will see examples of this where the Penrose diagrams for both Minkowski space and anti-de Sitter space will be regions of the static Einstein universe.

A conformal isometry is in a way similar to the symmetry that arises from a Killing vector field. As we saw above, moving along the orbits of a Killing vector field will not change the metric. That is, lengths between points are preserved. If the vector field is instead associated with a conformal isometry, moving along its orbits will not preserve lengths but it will preserve the light cone structure of the spacetime. This difference shows up in the right hand side of equation (2.1) as

$$\pounds_\xi g_{ab} = f g_{ab}, \tag{2.20}$$

where f is some function. In chapter 5 we will see examples of spacetimes that have conformal isometries.

It is also helpful to look at the Weyl tensor, which is the traceless part of the Riemann tensor. The Weyl tensor is given by[5]

$$C_{abcd} = R_{abcd} + \left(g_{a[d}R_{c]b} + g_{b[c}R_{d]a}\right) + \frac{1}{3}Rg_{a[c}g_{d]b}, \tag{2.21}$$

where square brackets stand for the totally antisymmetric part of that tensor. The Weyl tensor is conformally invariant. As we will see an example of later, if the Weyl tensor of a metric vanishes, the metric is conformally flat.

This knowledge will come in handy when we consider conformally compactified diagrams of spacetimes in chapter 3 as well as when we explore the conformal isometry of the charged black hole in a cosmological background in chapter 5.

Chapter 3

Anti-de Sitter space

As was mentioned in the introduction, the limit spacetimes of the charged or spinning black holes involve some variants of anti de-Sitter space. Due to this we will dedicate some time to discussing some relevant properties of these spaces and see how they arise in general relativity.

As Hawking and Ellis point out, spacetime metrics of constant curvature are locally characterized by the condition[5]

$$R_{abcd} = \frac{1}{12}\left(g_{ac}g_{bd} - g_{ad}g_{bc}\right)R, \tag{3.1}$$

This is equivalent to the traceless Ricci tensor and the Weyl tensor, defined by equation (2.21), vanishing

$$C_{abcd} = 0 = R_{ab} - \frac{1}{4}g_{ab}R, \tag{3.2}$$

as can be seen from its definition. In fact, by rearranging equation (2.21) we see that it splits the Riemann tensor into its three irreducible parts. That is, the Riemann tensor is split into terms containing the Weyl tensor, the traceless Ricci tensor and the scalar curvature. This means that the Riemann tensor of spacetimes with constant curvature is completely determined by the Ricci scalar. It follows from the equations above and the contracted Bianchi identities

$$R^{a}{}_{c;a} = \frac{1}{2}R_{;c}, \tag{3.3}$$

that R is constant in the whole spacetime as expected. We see that the Einstein tensor becomes

$$G_{ab} = R_{ab} - \frac{1}{2}g_{ab}R = -\frac{1}{4}Rg_{ab}, \tag{3.4}$$

which means that one can interpret these spacetimes as vacuum solutions of the field equations (1.3) with a cosmological constant $\lambda = \frac{1}{4}R$. If $R = 0$ we obtain the familiar Minkowski space, if $R > 0$ we obtain de Sitter space which we will not discuss and if $R < 0$ we obtain anti-de Sitter space which we are interested in. That is, anti-de Sitter space, adS, is a solution to Einstein's equations, (1.3), with a negative cosmological constant. The topology of adS_n is $S^1 \times R^{n-1}$ and can be visualized as the quadric

$$x_1^2 + x_2^2 + \ldots + x_{n-1}^2 - u^2 - v^2 = -1, \tag{3.5}$$

embedded in a $n+1$-dimensional flat space with the metric

$$ds^2 = dx_1^2 + dx_2^2 + \ldots + dx_{n-1}^2 - du^2 - dv^2. \tag{3.6}$$

The cases when $n = 2$ or $n = 3$ are of special interest to us in this thesis so we will discuss them further. When $n = 2$, the surface becomes a hyperboloid as is shown in figure 3.1. The three-dimensional case will be discussed in section 3.1 as we will be looking at a very special case of that spacetime.

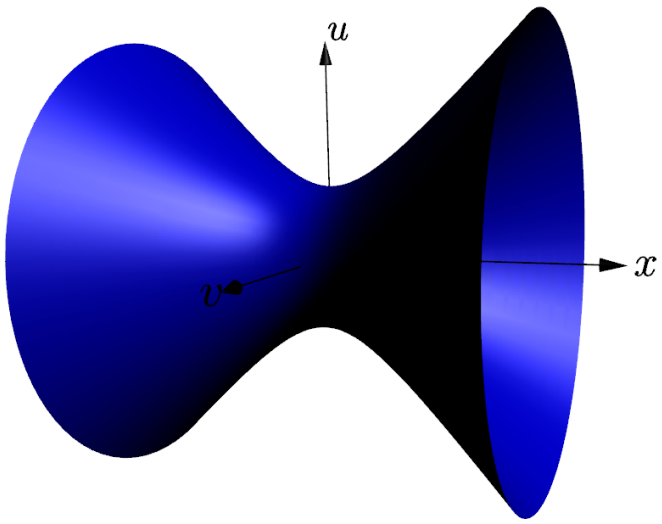

Figure 3.1: adS_2 depicted as a hyperboloid embedded in three-dimensional Minkowski space. Only in this $1+1$ dimensional case is the embedding space Minkowski space as is clear from equation (3.6).

For the two-dimensional case, we can define new coordinates, a and b, by

$$x = \sqrt{1+a^2}\cosh b, \qquad u = \sqrt{1+a^2}\sinh b, \qquad v = a, \tag{3.7}$$

which put the metric in the form

$$ds^2 = -(1+a^2)db^2 + \frac{da^2}{1+a^2}, \tag{3.8}$$

which is one of the forms we will recognize as adS_2 later in this thesis. As we will see, the different limits we look at in chapter 5 will cover different regions of the hyperboloid in figure 3.1. The coordinate transformation in (3.7) only cover half of the hyperboloid since x is always positive. We will see different representations of adS_2 in chapter 5.

3.1 Squashed or stretched

Even and odd dimensional spheres are considerably different. For our discussion, the most important difference is known as the *hairy ball theorem*[6], which tells us that on even dimensional spheres, it is impossible to a find a nowhere vanishing vector field. However, for odd dimensional spheres it is possible to find such vector fields. This means that odd dimensional spheres, and in particular S^3, can be squashed along these vector fields[7]. Squashing can be pictured as shrinking the spacetime along these particular vector fields. We are not restricted to simply squashing as we will see later, we can also stretch. In the same manner, it is possible to squash or stretch three-dimensional anti-de Sitter space along fibres that are space-, timelike or null[8]. For our purposes we will stick to spacelike squashing. We are interested in this very special variant of adS_3 as it turns out that one of the limit spacetimes we will deal with in chapter 6 is squashed anti-de Sitter space.

Equation (3.5) with $n = 3$ tells us that adS_3 is defined as the quadric

$$x^2 + y^2 - u^2 - v^2 = -1,$$

embedded in a flat four-dimensional space with the metric

$$ds^2 = dx^2 + dy^2 - dy^2 - dv^2.$$

We can represent this as the group manifold of $SL(2,\mathbb{R})$, in other words, matrices of the form

$$g = \begin{pmatrix} v+x & y+u \\ y-u & v-x \end{pmatrix},$$

with determinant one.

We can generate three everywhere non-vanishing Killing vectors by acting on g from the left with the matrices[1],

$$\sigma_1 = \begin{pmatrix} 1 & 0 \\ 0 & -1 \end{pmatrix}, \qquad \sigma_2 = \begin{pmatrix} 0 & 1 \\ 1 & 0 \end{pmatrix}, \qquad \sigma_0 = \begin{pmatrix} 0 & -1 \\ 1 & 0 \end{pmatrix},$$

which gives

$$\begin{aligned} J_1 &= -x\partial_u - u\partial_x - y\partial_v - v\partial_y, \\ J_2 &= -x\partial_v - v\partial_x + y\partial_u + u\partial_y, \\ J_0 &= -x\partial_y + y\partial_x + u\partial_v - v\partial_u. \end{aligned} \tag{3.9}$$

From $Tr(dgg^{-1}) = 0$, we find that

$$dgg^2 = \Sigma\sigma_i\theta_i. \tag{3.10}$$

Solving these equations for θ_i gives

$$\begin{aligned} \theta_1 &= -udx - vdy + xdu + ydv, \\ \theta_2 &= -vdx + udy - ydu + xdv, \\ \theta_3 &= -ydx + xdu - vdu + udv, \end{aligned} \tag{3.11}$$

known as the Maurer-Cartan forms. Notice that $\theta_i(J_j) = \delta_{ij}$.

We introduce new coordinates τ, ω and σ such that

$$\begin{aligned} g &= e^{\tau\sigma_0/2}e^{\omega\sigma_2/2}e^{-\sigma\sigma_1/2} \\ &= \begin{pmatrix} \cos\frac{\tau}{2} & -\sin\frac{\tau}{2} \\ \sin\frac{\tau}{2} & \cos\frac{\tau}{2} \end{pmatrix} \begin{pmatrix} \sinh\frac{\omega}{2} & \cosh\frac{\omega}{2} \\ -\cosh\frac{\omega}{2} & -\sinh\frac{\omega}{2} \end{pmatrix} \begin{pmatrix} e^{-\sigma/2} & 0 \\ 0 & e^{\sigma/2} \end{pmatrix}. \end{aligned} \tag{3.12}$$

We can expand these matrices and compare to g calculated in terms of x,y,u and v from equations (3.10) and (3.11) to find

[1]Acting from the right would give three more Killing vectors, making the dimension of the isometry group six, $SL(2,\mathbb{R}) \times SL(2,\mathbb{R})$ but we don't need them for the following calculation so their exact forms will be skipped.

$$
\begin{aligned}
x &= \cos\frac{\tau}{2}\sinh\frac{\omega}{2}\cosh\frac{\sigma}{2} - \sin\frac{\tau}{2}\cosh\frac{\omega}{2}\sinh\frac{\sigma}{2},\\
y &= \sin\frac{\tau}{2}\sinh\frac{\omega}{2}\cosh\frac{\sigma}{2} + \cos\frac{\tau}{2}\cosh\frac{\omega}{2}\sinh\frac{\sigma}{2},\\
u &= \cos\frac{\tau}{2}\cosh\frac{\omega}{2}\cosh\frac{\sigma}{2} + \sin\frac{\tau}{2}\sinh\frac{\omega}{2}\sinh\frac{\sigma}{2},\\
v &= \sin\frac{\tau}{2}\cosh\frac{\omega}{2}\cosh\frac{\sigma}{2} - \cos\frac{\tau}{2}\sinh\frac{\omega}{2}\sinh\frac{\sigma}{2},
\end{aligned}
\tag{3.13}
$$

and in terms of these new coordinates, the θ_i can be written as

$$
\begin{aligned}
\theta_1 &= \frac{1}{2}\left(\sinh\sigma\cosh\omega d\tau - \cosh\sigma d\omega\right),\\
\theta_2 &= \frac{1}{2}\left(\sinh\omega d\tau + d\sigma\right),\\
\theta_0 &= \frac{1}{2}\left(\cosh\omega\cosh\sigma d\tau - \sinh\sigma d\omega\right).
\end{aligned}
$$

Up to a constant, the metric is given by[7]

$$
\begin{aligned}
ds^2 &= Tr(dgg^{-1}dgg^{-1})\\
&= -\theta_0^2 + \theta_1^2 + \theta_2^2\\
&= \frac{1}{4}\left(-\cosh^2\omega d\tau^2 + d\omega^2 + \left(d\sigma + \sinh\omega d\tau\right)^2\right),
\end{aligned}
$$

which we can squash or stretch along J_2

$$
ds^2 = \frac{1}{4}\left(-\cosh^2\omega d\tau^2 + d\omega^2 + \alpha^2\left(d\sigma + \sinh\omega d\tau\right)^2\right),
\tag{3.14}
$$

where α is the squashing or stretching parameter. It is less than one when squashing and larger than one when stretching.

Let us look at what happens to the Killing vectors when we squash or stretch. Writing the Killing vectors in terms of τ, ω and σ gives[9]

$$
\begin{aligned}
J_1 &= -\frac{2\sinh\sigma}{\cosh\omega}\partial_\tau - 2\cosh\sigma\partial_\omega + 2\tanh\omega\sinh\sigma\partial_\sigma,\\
J_2 &= 2\partial_\sigma,\\
J_0 &= \frac{2\cosh\sigma}{\cosh\omega} + 2\sinh\sigma\partial_\omega - 2\tanh\omega\cosh\sigma\partial_\sigma.
\end{aligned}
$$

We can check how the isometry group changes under this squashing or stretching. To do this, we look at the Lie derivative of the metric with

respect to each Killing vector and see if it vanishes as it did before we squashed or stretched

$$\begin{aligned}\pounds_\xi g_{ab} &= \xi_{a;b} + \xi_{b;a} \\ &= \partial_a \xi_b + \partial_b \xi_a - 2\xi_c \Gamma_{ab}{}^c,\end{aligned}$$

which is zero for J_2 as can be seen from the Christoffel symbols for the metric (3.14) since $(J_2)_i \Gamma^i{}_{ab} = 0$, where i is any pair combination of τ, ω and σ. However, J_1 and J_0 have a few non-zero elements

$$\begin{aligned}\pounds_{J_1} g_{\tau\omega} &= -\frac{1}{2}\sinh\sigma\sinh\omega\left(1-\alpha^2\right), \quad \pounds_{J_0} g_{\tau\omega} = \frac{1}{2}\cosh\sigma\sinh\omega\left(1-\alpha^2\right), \\ \pounds_{J_1} g_{\tau\sigma} &= -\frac{1}{2}\cosh\sigma\cosh\omega\left(1-\alpha^2\right), \quad \pounds_{J_0} g_{\tau\sigma} = \frac{1}{2}\sinh\sigma\cosh\omega\left(1-\alpha^2\right), \\ \pounds_{J_1} g_{\omega\sigma} &= -\frac{1}{2}\sinh\sigma\left(1-\alpha^2\right), \qquad \pounds_{J_0} g_{\omega\sigma} = \frac{1}{2}\cosh\sigma\left(1-\alpha^2\right),\end{aligned}$$

so we see that J_1 and J_0 are no longer Killing vectors if $\alpha \neq 1$, that is they only remain Killing vectors if there is no squashing or stretching at all. Since the other three Killing vectors (the ones "from the right") are not affected by this, they obviously remain Killing vectors. It now follows that the isometry group is four dimensional, as opposed to six as it was before squashing or stretching. It also remains a homogeneous space in the sense that any point in the space can be reached by moving only along Killing vector fields.

Chapter 4

Carter-Penrose diagrams

Since the spacetimes we will be working with in this thesis are typically of dimensions higher than two, it is beneficial to conformally compactify them into a two-dimensional picture that captures the causal structure of the original spacetime, a so called *Carter-Penrose diagram*. This means that it is possible to attach a boundary to this picture which captures the idea of asymptotically flat spacetimes, as discussed in chapter 1. In general, if the cosmological constant is non-vanishing the picture captures the asymptotic behaviour of the gravitational field. We will see that these diagrams capture the causal structure of the original spacetime due to the results from chapter 2. Namely, it will turn out that these diagrams are regions of an unphysical spacetime that is conformal to the original spacetime so we see that they share the same causal structure.

If the spacetime is spherically symmetric, we know that every point in the spacetime sits on a round sphere. This means we can let each point in the conformally compactified picture represent an entire round sphere, so that the picture becomes two-dimensional. These diagrams will show us the most important features of the original spacetime while remaning very simple.

We start by drawing the Carter-Penrose diagram for (four-dimensional) Minkowski space and then move on to more complicated things. As we know the metric for Minkowski space is

$$ds^2 = -dt^2 + dr^2 + r^2 d\Omega_2^2, \tag{4.1}$$

where $d\Omega_2^2$ is the metric of the two-sphere. Making the range of coordinates finite by defining p and q as

$$\tan p = t - r, \qquad \tan q = t + r, \tag{4.2}$$

the Minkowski metric becomes

$$d\hat{s}^2 = \frac{1}{4\cos^2 p \cos^2 q}\left(-4dpdq + \sin^2(p-q)\, d\Omega_2^2\right), \tag{4.3}$$

which we can conformally scale to get rid of the infinity at $\cos q$ or $\cos p$ equal to zero. This means that the conformally scaled metric is now

$$\begin{aligned} ds^2 &= \Omega^2 d\hat{s}^2 \\ &= -4dpdq + \sin^2(p-q)\, d\Omega_2^2. \end{aligned} \tag{4.4}$$

Changing coordinates one last time with

$$\tau = p + q, \qquad\qquad \rho = q - p, \tag{4.5}$$

puts the metric in the form

$$ds^2 = -d\tau^2 + d\rho^2 + \sin^2\rho d\Omega_2^2, \tag{4.6}$$

which is the static Einstein universe. We see that it has the topology of R times a sphere, where the spheres are round and do not change with time. From equation (4.5) and the fact that p and q range between $-\pi/2$ and $\pi/2$, we see that

$$-\pi < \tau + \rho < \pi, \qquad -\pi < \tau - \rho < \pi, \qquad \rho \geq 0. \tag{4.7}$$

As promised in chapter 2, Minkowski space is conformal to a finite region of the static Einstein universe, defined by the restrictions (4.7). Here the term unphysical spacetime from chapter 2 becomes clear as we see that while on its own, the static Einstein universe is perfectly physical, the region which is not covered by the coordinates in equation (4.7) is unphysical with respect the original Minkowski space as it lies beyond infinity in a sense. From this we draw the Carter-Penrose diagram of Minkowski space in figure 4.1b as half of the region depicted in figure 4.1a.

The different points and surfaces on the figures are

- i^-: past timelike infinity, given by $\tau = -\pi$ and $\rho = 0$,
- i^+: future timelike infinity, given by $\tau = \pi$ and $\rho = 0$,
- i^0: spatial infinity, given by $\tau = 0$ and $\rho = \pi$,
- $\mathscr{I}^-$: past null infinity, given by $\tau = -\pi + \rho$ for $0 < \rho < \pi$,
- $\mathscr{I}^+$: future null infinity, given by $\tau = \pi - \rho$ for $0\rho < \pi$.

From this we see that all timelike geodesics begin at i^- and end at i^+, all spacelike geodesics begin and end at i^0 and all null geodesics begin at $\mathscr{I}^-$ and end at $\mathscr{I}^+$. These terms will show up again in the Carter-Penrose diagrams for other spacetimes.

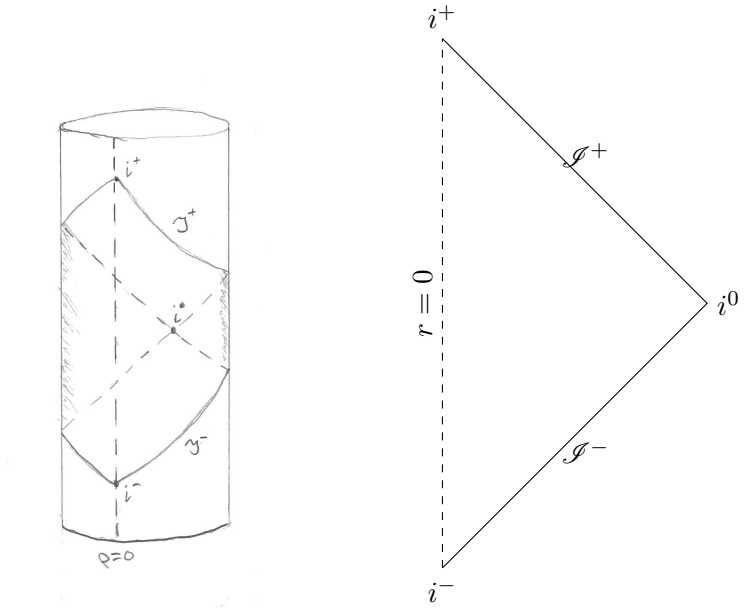

(a) The static Einstein universe

(b) The Carter-Penrose diagram

Figure 4.1: The static Einstein universe with the region defined by (4.7) and the corresponding Carter-Penrose diagram. Notice that $r = 0$ and $\rho = 0$ are the same curves. In figure 4.1b each point represents a sphere except the dashed line where the sphere has shrunk to radius zero and therefore points are simply points. We note that if figure 4.1a is taken to show a $1+1$ dimensional Einstein universe each point represents a point. However, if figure 4.1b is taken to show a $1+1$ dimensonal Minkowski space each point (except those on the dashed line) represents a pair of points, but we know that a pair of points is the zero-dimensional sphere, S^0.

The Carter-Penrose diagram for anti-de Sitter space can be obtained in a similar way. The metric

$$d\bar{s}^2 = -\cosh^2 r d\tau^2 + dr^2 + \sinh^2 r d\Omega_2^2, \tag{4.8}$$

covers the whole of four-dimensional anti-de Sitter space[5]. If we introduce a new coordinate ρ such that

$$\rho = 2\tan^{-1}(e^r) - \frac{\pi}{2}, \tag{4.9}$$

which means that $0 \leq \rho \leq \frac{\pi}{2}$. Using the following identities

$$\frac{dr}{d\rho} = \frac{1}{\cos\rho}, \qquad \cosh r = \frac{1}{\cos\rho}, \qquad \sinh r = \frac{\sin\rho}{\cos\rho}, \tag{4.10}$$

we can write the metric in the following form

$$d\bar{s}^2 = \cos^{-2}\rho ds^2, \tag{4.11}$$

where ds^2 is given by equation (4.6) and $d\bar{s}^2$ by equation (4.8). Just as for the Minkowski spacetime, we see that anti-de Sitter space is conformal to a region of the static Einstein universe, in particular the region where $0 \leq \rho \leq \pi/2$. We draw its Carter-Penrose diagram in figure 4.2b as half of the region depicted in figure 4.2a. Notice that $\mathscr{I}$ is timelike rather than lightlike as it is for Minkowski space. In fact, it can be proven[10] that $\mathscr{I}$ is a timelike hypersurface when $\lambda < 0$, a spacelike hypersurface when $\lambda > 0$ and a null hypersurface when $\lambda = 0$. As was mentioned before, notice that the hypersurface $\mathscr{I}$ in figure 4.2b is an ordinary hypersurface in the static Einstein universe defined by $\rho = \pi/2$, or $\Omega = 0$ since $\rho = \pi/2$ corresponds to $r = \infty$ as is clear from equation (4.9).

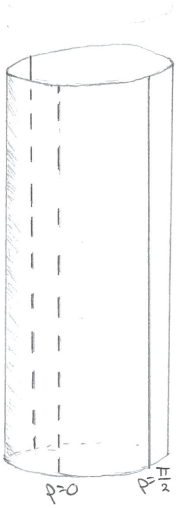

(a) The static Einstein universe.

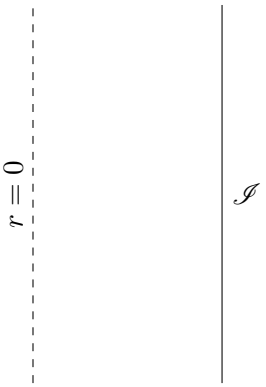

(b) The Carter-Penrose diagram

Figure 4.2: The static Einstein universe and the region defined by $0 \leq \rho \leq \frac{\pi}{2}$ and the corresponding Carter-Penrose diagram. As for Minkowski space, we see from equation (4.9) that $r = 0$ and $\rho = 0$ are the same curve. Remember that each point in figure 4.2b is a sphere, except the points on the dashed line as before.

For black hole spacetimes, the coordinate transformations required to bring the metric to a conformal form such as the metric (4.6) are a bit more involved. Therefore it is beneficial to introduce block diagrams, as discussed by Walker in [11]. Due to the nature of Carter-Penrose diagrams we will only consider spherically symmetric black holes. That is, we work with an interesting case of a spherically symmetric, static two-surface with a metric of the form

$$ds^2 = -Vdt^2 + dr^2/V, \tag{4.12}$$

where V is the norm of the timelike Killing vector of the metric and has n roots. This surface is totally geodesic. That is, any geodesic on this surface is also a geodesic in the full spacetime. V is a function of r and could be a function of the other coordinates on the rest of spacetime as well, but due to being totally geodesic we know that the other coordinates can be chosen to be constant on this surface.

When V vanishes, the orbits of the Killing vector become null so one can think of the roots splitting the spacetime into $n + 1$ regions. These regions can be bounded by three different cases. Either two of the null orbits, one

null orbit and $\mathscr{I}$ or a null orbit and a singular line, which is defined as a point where both V and the Gaussian curvature,

$$K = \frac{1}{2}\frac{d^2V}{dr^2}, \tag{4.13}$$

become unbounded. In terms more related to the rest of this thesis, these three cases correspond to being bounded by two horizons, a horizon and infinity or a horizon and a curvature singularity, respectively. These blocks can then be glued together along nonsingular boundaries, called *seams*, to create Carter-Penrose diagrams. It turns out that the timelike coordinate in each block changes vertically and that the Gaussian curvature, K, must be smooth across the seam between two blocks, which as Walker points out, means that a block cannot be flipped and joined to itself. Blocks bounded by two horizons or a horizon and $\mathscr{I}$ where the block is asymptotically flat take the shape of a diamond while blocks bounded a horizon and a singular line or a horizon and $\mathscr{I}$ where the block is not asymptotically flat take the shape of a triangle.

As an example, we will draw the Carter-Penrose diagram for the Schwarzschild metric given by equation (1.4). Here each point represents a sphere with no exceptions since the topology of the maximally extended Schwarzschild solution is R^2 times S^2, as opposed to R^4 for the Minkowski case.

Now, $V = 1 - \frac{2m}{r}$ which has one zero at $r = 2m$. So there are two blocks that we can draw. We start by drawing a block, T_1, which is bounded by a horizon and $\mathscr{I}$. Since the Schwarzschild spacetime is asymptotically flat this will be a diamond. The second block, T_2, is bounded by a horizon and a singular line, meaning that it will be a triangle. We glue the two blocks together along their common seams, the horizon, and draw figure 4.4. On the figure, the maximal analytical extension of the spacetime has been drawn in red. This is done by gluing together the blocks in every possible way. In our case, we turn T_2 up side down and glue it along the lower seam on T_1 and add a second T_1 block to the left of the two T_2 blocks which is mirrored compared to the other T_1 block.

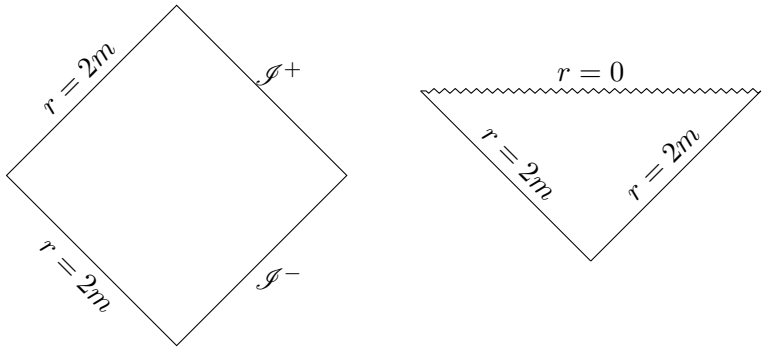

(a) T_1 (b) T_2

Figure 4.3: The blocks of the Schwarzschild spacetime.

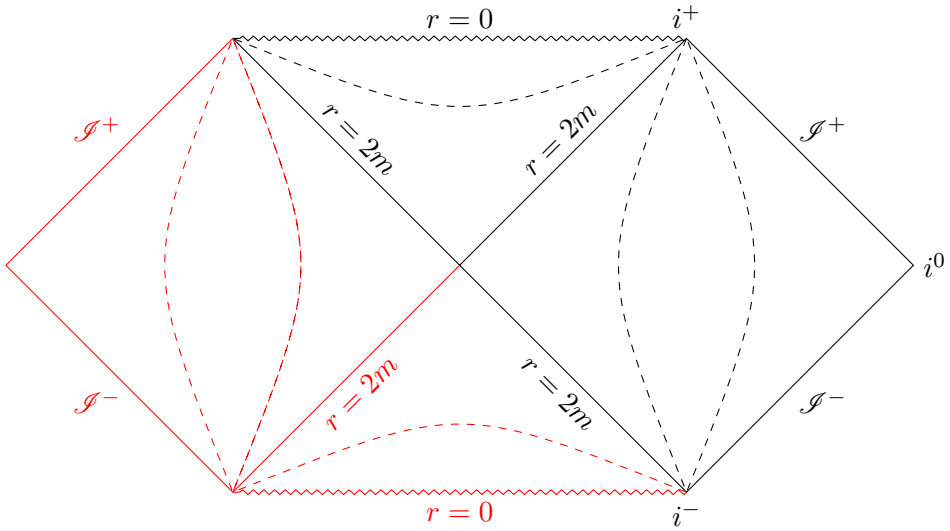

Figure 4.4: Carter-Penrose diagram for the Schwarzschild black hole. The red lines indicate the maximal extension of the spacetime. The dashed lines are surfaces of constant r.

Chapter 5

Reissner-Nordström - a charged black hole

The first black hole we will consider is the charged black hole. A spherical charged black hole is described by the Reissner-Nordström metric,

$$ds^2 = -V(r)dt^2 + \frac{dr^2}{V(r)} + r^2 d\Omega_2^2, \tag{5.1}$$

where

$$V(r) = \frac{(r - r_+)(r - r_-)}{r^2} \tag{5.2}$$

and

$$r_\pm = m \pm \sqrt{m^2 - e^2}, \tag{5.3}$$

and $d\Omega_2^2$ is the metric of the two-sphere. It is clear that putting the charge, e, to zero will give the Schwarzschild metric as given by equation (1.4). This spacetime has two horizons positioned at r_- and r_+. We notice that if $e^2 > m^2$, $r_\pm$ turn imaginary and there would be no horizons. This case will not be considered as we are only interested in spacetimes with horizons.

Just as for the Schwarzschild metric, the singularity at $r = 0$ is the curvature singularity. The Killing vector fields for the charged black hole are the same as that of the Schwarzschild black hole[12] as given in chapter 2.

When $e^2 = m^2$ the black hole is extremal, it has the maximum available charge while remaining a black hole. As was mentioned in chapter 2, while this is a convenient way to see whether a black hole is extremal or not, it is not exactly correct. As we will see in section 5.3, a black hole that has

$e^2 = m^2$ sitting in a cosmological background will not be extremal as the proper definition of an extremal black hole is a black hole that has zero surface gravity. That is, its Killing horizon is degenerate.

Turning back to the extremal black hole, we notice that there is only one degenerate horizon, sitting at $r = m$, as was expected. That this happens is easily verified in equation (5.3). This changes the spacetime in various ways. The most obvious change is that g_{tt} and g_{rr} no longer change sign when crossing the horizon as they do in the non-extremal case so t and r are always time- and spacelike coordinates respectively. Another peculiar feature of this extremal spacetime is that if we calculate the distance along a spacelike curve from a point sitting at $r_0 > r_+$ and to the horizon it turns out to be infinite. Therefore it is of interest to look at how the spacetime changes when close to the horizon.

Following the prescription for drawing Carter-Penrose diagrams from section 4, we draw figure 5.1a for the metric (5.1). However, we see that the two horizons split the spacetime into three blocks, or regions. Since the horizon is degenerate when $e^2 = m^2$, we see that region II has disappeared since it was defined as the region between the two horizons. Drawing a diagram corresponding to the black region of figure 4.4 for the extremal Reissner-Nordström black hole shows this. That is, figure 5.1b only has regions I and III.

To look at this further, we can calculate the distance between r_- and r_+ (in the non-extremal case). That is, we can calculate the length of a timelike curve at constant θ, ϕ and t

$$L = -\int_{r_+}^{r_-} dr \, \frac{r}{\sqrt{(r - r_+)(r - r_-)}} = \pi m, \tag{5.4}$$

and we see that the distance between r_- and r_+ is a constant which does not depend on e[13]. This seems to go against the fact that the two null hypersurfaces, $r_\pm$, coincide for the extremal black hole. On one hand the two null hypersurfaces, $r_\pm$, coincide and therefore from figure 5.1b the length calculated in equation (5.4) seems to disappear, or become a null curve. But on the other hand, equation (5.4) suggests that it does not vanish. This tells us that we should take care when discussing and calculating things that have to do with these two hypersurfaces in the scaling limit, as we do below.

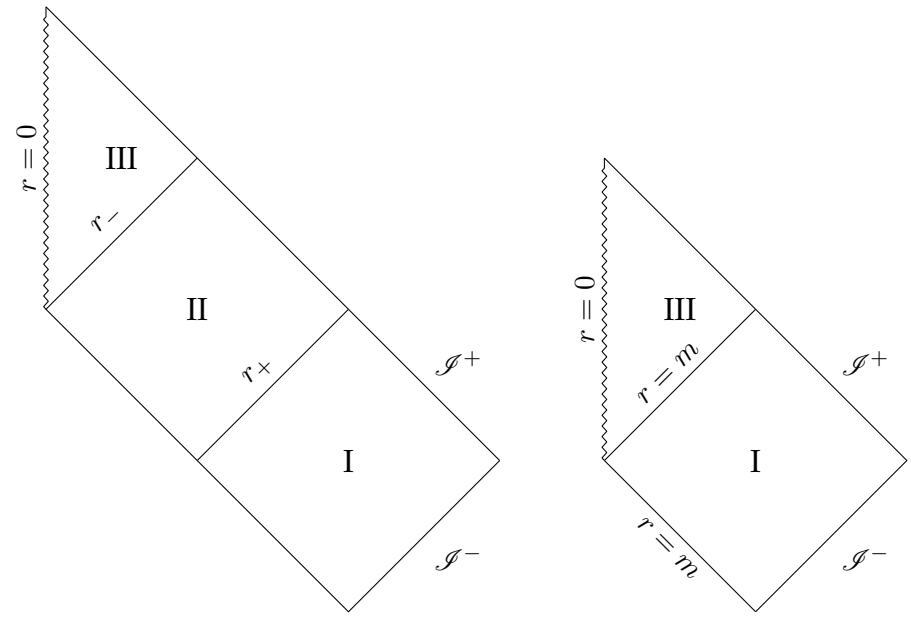

(a) Non-extremal (b) Extremal

Figure 5.1: Carter-Penrose diagram for both the non-extremal (a) and the extremal (b) Reissner-Nordström black hole.

5.1 Near-horizon

We want to look closely at the geometry close to the horizon of an extremal charged black hole. We know that the metric is still given by equation (5.1), but now $V(r)$ is

$$V(r) = \frac{(r-m)^2}{r^2}, \tag{5.5}$$

which has a single horizon at $r = m$ as was mentioned above. We are interested in looking at the limit $r \to m$, but just as for the Schwarzschild limits, we need to define new coordinates that allow the limit to be taken more clearly,

$$r = m + \varepsilon\chi, \qquad\qquad t = m^2\frac{\psi}{\varepsilon}, \tag{5.6}$$

where ε is a dimensionless parameter that goes towards zero as we zoom in on the horizon. Note that the limit $r \to m$ is now $\varepsilon \to 0$. Doing these coordinates changes and taking the limit, the metric becomes

$$ds^2 = m^2\left(-\chi^2 d\psi^2 + \frac{1}{\chi^2}d\chi^2 + d\Omega_2^2\right), \tag{5.7}$$

which is the product of two-dimensional anti de-Sitter space and a two-sphere of constant radius, $adS_2 \times S^2$. This metric is an electrovac solution to the Einstein-Maxwell equations called the Bertotti-Robinson solution. We see that hypersurfaces at constant ψ, which are in a sense constant time hypersurfaces, are infinitely long cylinders.

However, these coordinates do not cover the whole adS_2 spacetime. To find out which region of adS_2 they cover, we use that adS_2 is defined as the quadric,

$$x^2 - u^2 - v^2 = -1, \tag{5.8}$$

embedded in a space with the metric

$$ds^2 = dx^2 - du^2 - dv^2. \tag{5.9}$$

Defining y and t such that $x_+ = 1/y$ and $v = \psi/y$ where $x_\pm = x \pm u$ and using equations (5.8) and (5.9) the metric becomes

$$ds^2 = \frac{1}{y^2}\left(-d\psi^2 + dy^2\right), \tag{5.10}$$

if we now define $y = 1/\chi$, this becomes the same metric as above. We see that in the coordinate transformation y cannot be zero and thus we have to make a choice whether it is positive or negative. Since x_+ is simply the inverse of y we see that it carries the same sign so the choice of y translates to $x + u$ being either positive or negative in the embedding space. In figure 5.2 the hyperboloid defined by equation (5.8) has been drawn in blue along with the plane $x + u = 0$ in green. Depending on the choice of y, the region of adS_2 that this metric covers is on either side of this green plane. If y is positive, then so is $x+u$ and therefore the region of adS_2 are those points in the embedding space that sit on the hyperboloid defined by equation (5.8) and lie above the plane $x + u = 0$. The opposite holds if y is chosen to be negative, the points would lie below the plane $x + u = 0$. We notice that the plane $x + u = 0$ splits the hyperboloid of figure 5.2 in half so the metric (5.7) covers half adS_2 space.

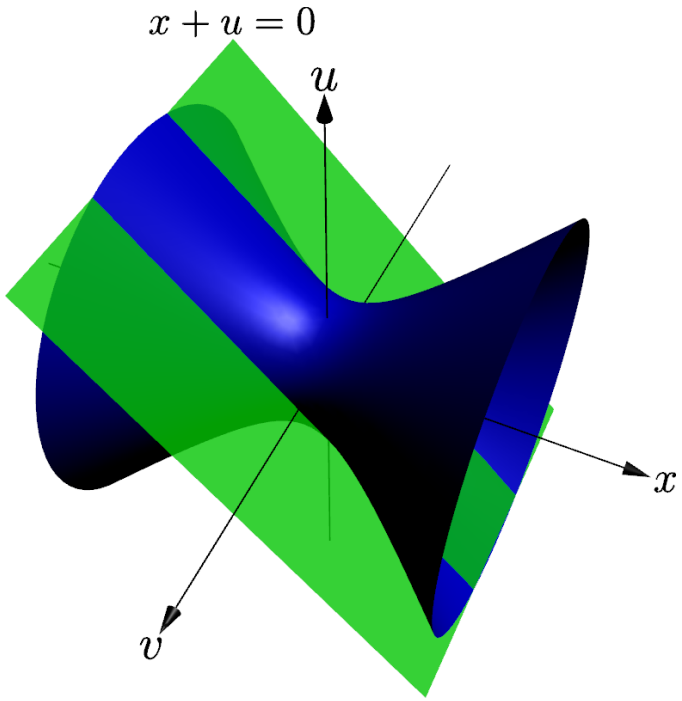

Figure 5.2: Plot of x, u and v, showing which piece of the diagram the metric (5.10) covers. The region is the part of the blue surface that is above the green surface if y was chosen to be positive and below if negative.

In figure 5.3 we show a Carter-Penrose diagram of the Bertotti-Robinson spacetime. Since time is periodic, we see very clearly that only half of the spacetime is covered.

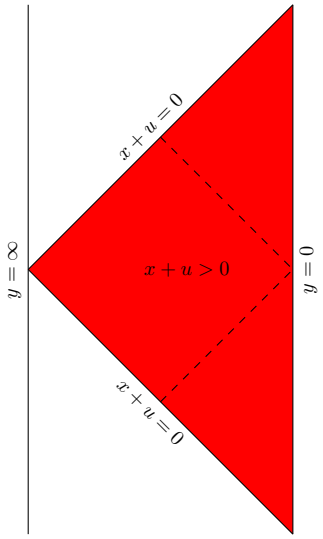

Figure 5.3: Plot of ψ and y, showing how the condition on $x+u$ translates to this diagram. Notice that we are not looking at an infinitely long strip as we assume that time is periodic.

An interesting feature of the metric (5.10) and also the metric (5.7) is that it is conformally flat. That is, we can rewrite, after defining $\chi = 1/y$, the latter metric as

$$\begin{aligned} ds^2 &= \frac{m^2}{y^2}\left(-d\psi^2 + dy^2 + y^2 d\Omega_2^2\right), \\ &= \frac{m^2}{y^2} ds^2_{\text{flat}}, \end{aligned} \tag{5.11}$$

where ds^2_{flat} is the metric of flat space. In physical terms, this means that the region close to the horizon of an extremal black hole is conformal a neighbourhood around $\mathscr{I}$. This means that the light cone structure of the near-horizon geometry is that of flat space.

The extremal charged black hole has a conformal isometry before taking the near-horizon limit. As Couch and Torrence showed[14], if we define a new coordinate $x' = -m/(r-m)$ in the original metric (5.1) with (5.2) as $V(r)$, the transformation $x = 1/x'$ is a conformal transformation. That is,

$$\begin{aligned} ds^2 &= \frac{dt^2}{(x'-1)^2} - m^2\left(x'-1\right)^2 \frac{dx'^2}{x'^4} - \frac{m^2\left(x'-1\right)^2}{x'^2} d\Omega_2^2, \\ &= x^2\left(\frac{dt^2}{(x-1)^2} - m^2\left(x-1\right)^2 \frac{dx^2}{x^4} - \frac{m^2\left(x-1\right)^2}{x^2} d\Omega_2^2\right). \end{aligned} \tag{5.12}$$

We see that it is an inversion in the sense that it interchanges the event horizon, H, and null infinity, $\mathscr{I}$. In preparation for what is to come, it is worth mentioning that this conformal isometry acts as a reflection around the surface $r = 2m$ since $x(2m) = -1$ and is mapped into itself. It is therefore not a continuous isometry but a discrete one. As Brännlund pointed out in [15] such a conformal isometry also exists in a special case when a non-zero cosmological constant is present. This will be discussed in detail in section 5.3.

5.2 $e \to m$ scaling limit

It is possible to take the near-horizon limit in a different manner. Rather than making the black hole extremal and then taking the near-horizon limit, these two steps can be taken simultaneously for the whole spacetime. As we are now focusing on the whole spacetime, not just the region close to the horizon, we switch to Eddington-Finkelstein coordinates[1] that are non-singular at the horizon(s), defined by

$$\eta = t + r_*, \qquad\qquad r_* = \int dr\, \frac{1}{V(r)}, \tag{5.13}$$

where $V(r) = \frac{(r-r_+)(r-r_-)}{r^2}$. In these coordinates the metric becomes

$$ds^2 = -V(r)d\eta^2 + 2d\eta dr + r^2 d\Omega_2^2. \tag{5.14}$$

A coordinate transformation identical to the transformation from equation (5.6), with η replacing t, will serve for this limit as well. However this time around, the parameter ε is now defined as

$$\varepsilon = \sqrt{m^2 - e^2}, \tag{5.15}$$

such that it goes to zero in the limit $e^2 \to m^2$. This limit was considered by Carroll et al[13], but done separately for each of the three regions. Using the coordinate transformations on the metric in equation (5.14) and letting $e^2 \to m^2$, we obtain

$$ds^2 = m^2 \left(-\left(\chi^2 - 1\right) d\psi^2 + 2d\psi d\chi + d\Omega_2^2 \right), \tag{5.16}$$

which as before is $adS_2 \times S^2$ but it is not the same region as in the near-horizon limit. The fact that we used the same coordinate transformation as before warrants some discussion. By using the same transformation,

[1]The suggestion to use these coordinates was made by José Senovilla.

we are not looking at a case analogous to the simple example in the introduction, where we had two different limits of the same spacetime depending on which coordinate transformation was done. Here we are looking at two different, but related ($e^2 = m^2$ and $e^2 \neq m^2$) spacetimes and taking two limits that in the physical sense mean different things but in the mathematical sense are represented by the same coordinate transformation. This is highlighted even further by the fact that the resulting spacetimes in all cases describe the geometry close to the horizon so both limits are in a sense a near-horizon limit while the one we call the scaling limit is more direct in a sense.

Turning back to which region of adS_2 the spacetime in equation (5.16) covers we must find a coordinate transformation from these coordinates to the embedding space and see which restrictions apply, just as in the near-horizon limit. Due to the behaviour at $\chi = \pm 1$, we must use different transformations in the different regions,

$$
\begin{aligned}
|\chi| > 1: \qquad & x = \pm\sqrt{\chi^2 - 1}\cosh\left(\psi - \chi_*\right), \\
& u = \pm\sqrt{\chi^2 - 1}\sinh\left(\psi - \chi_*\right), \qquad (5.17) \\
& v = \pm\chi \\
|\chi| < 1: \qquad & x = \pm\sqrt{1 - \chi^2}\sinh\left(\psi - \chi_*\right), \\
& u = \pm\sqrt{1 - \chi^2}\cosh\left(\psi - \chi_*\right), \qquad (5.18) \\
& v = \pm\chi,
\end{aligned}
$$

where χ_* is defined in an analogous way to r_* but with respect to the limit metric (5.16). All of these transformations, for different choices of the pluses and minuses give the metric (5.16) from the embedding metric. Note that the different plus and minus signs are not related and choosing one of them does not fix the others.

In equations (5.18) we choose the plus signs. By making this choice we only consider positive values of u in that region and this explains why we look down on the hyperboloid in figure 5.4a.

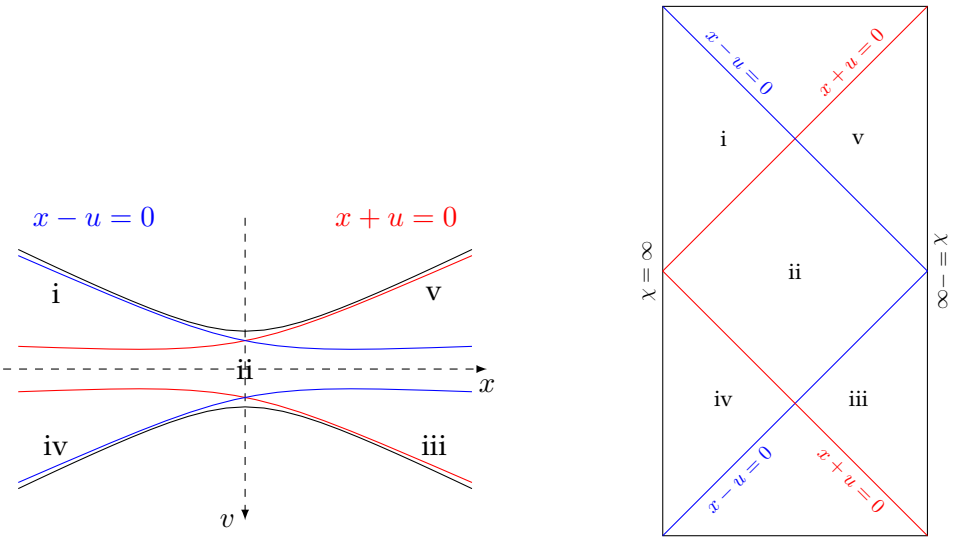

(a) The hyperboloid

(b) The Carter-Penrose diagram

Figure 5.4: The relationship between regions of the top down view of the hyperboloid and the conformal regions.

For $|\chi| > 1$, we have multiple choices. These choices are represented by the regions i, iii, iv and v in figures 5.4a and 5.4b. In principle, any two pairs of the four regions could be chosen, six in total. However, there is another restriction which narrows the choices we can make when selecting those regions. Before taking the scaling limit, the metric is given by (5.14). This metric has a null coordinate that extends through the whole spacetime. In terms of figure 5.4b, this means that this null coordinate can be drawn as a straight line going through the spacetime from minus infinity to infinity. Therefore if we want to keep this feature of the spacetime, we are limited to only two possible choices for the signs in equations (5.17) and (5.18), corresponding to ingoing or outgoing null coordinates. These choices correspond to the pairs (i,iii) and (iv,v), respectively. But from equation (5.13) we know that our null coordinate is ingoing and therefore we choose regions i and iii.

To get a better view of the hyperboloid we draw a figure similar to 5.2. This is shown in figure 5.5 and for completeness we also draw the Carter-Penrose diagram and color the regions coordingly in figure 5.6. From these we see that region I covers the part facing outwards in figure 5.5 but only for positive x, region II covers the part between the two surfaces but only for positive u and region III covers a similar part as region I but on the other side of the second surface and only for negative x, and as mentioned before, it only covers all of it in the scaling limit. From this we notice that in all three regions, due to the restrictions on x and u from equations (5.17)

and (5.18), these coordinates cover only half of the respective region. We conclude that the metric covers half of adS_2, but it is not the same half that is covered by the near-horizon limit, as was discussed above.

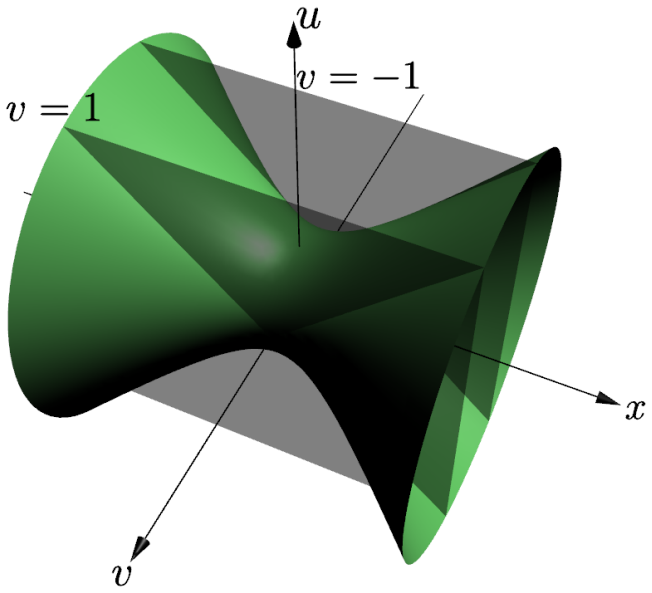

Figure 5.5: The three regions of the Carter-Penrose diagram in figure 5.1a. Region I for positive x and v, region II between the two surfaces and region III for negative x and v.

In figure 5.6 it is even clearer that half of adS_2 is covered. There the conformal version of adS_2 has been drawn and the three regions colored in red, green and blue.

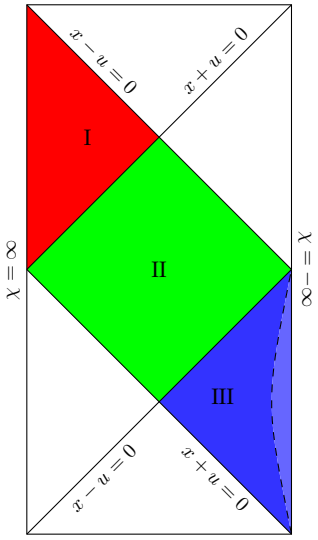

Figure 5.6: Regions I, II and III from figures 5.1 and 5.5 in a block diagram. The dashed line moves into the light blue area as e gets closer to m and concides with $\chi = -\infty$ once extremality is achieved.

Therefore we see that the scaling limit is very similar to the near-horizon limit. The main differences are that the region covered of adS_2 by the limit spacetime is different and that the calculation is done in one swoop rather than making the black hole extremal and then zooming in on the horizon. This is depicted schematically in figure 5.7. This figure explains what was discussed in the introduction, namely that we are not taking limits of the same spacetime, rather that we are taking limits of different spacetimes but the limit spacetime turns out to be the same.

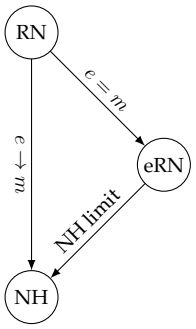

Figure 5.7: A schematic picture of the different limits for the charged (RN) black hole. The scaling limit ($e \to m$) is taken in one step while the near horizon limit (NH) has the extremal Reissner-Nordström black hole (eRN) as its starting point.

In figure 5.8 we look at the hyperboloid again from the top down. There we see clearly which parts of the hyperboloid are covered by which limit. The purple region is covered by both limits while the red region is only covered by the scaling limit and the blue region only by the near-horizon limit. These two regions correspond to regions i and iv in figure 5.4, respectively.

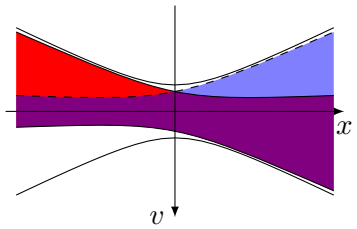

Figure 5.8: Looking down on the hyperboloid. The purple region is the common region of the two limits while the blue region only belongs to the near-horizon limit and the red region only to the scaling limit.

5.3 Reissner-Nordström de Sitter - a cosmological background

We now turn our attention towards slightly different things. If we put the charged black hole into a universe with positive curvature, we obtain the so called Reissner-Nordström de Sitter spacetime. It is still spherically symmetric and therefore the metric is given by (5.1) just like the charged black hole but with a different $V(r)$ given by

$$V(r) = 1 - \frac{2m}{r} + \frac{e^2}{r^2} - \frac{\lambda}{3}r^2, \tag{5.19}$$

where λ is the cosmological constant. By adding this new term, the metric terms g_{tt} and g_{rr} have picked up two new more roots, a total of four. One of them is unphysical, two of them are the usual Reissner-Nordström horizons and the last, and largest, is the cosmological horizon. Note that in a de Sitter spacetime without a black hole, there is still a cosmological horizon.

We know that the Hawking temperature of a horizon is given by[16]

$$T_H = \frac{\kappa}{2\pi}, \tag{5.20}$$

where κ is the surface gravity, defined by equation (2.17) in section 2.1.1. An interesting case for this black hole is when the temperatures of the outer black hole horizon, r_b, and the cosmological horizon, r_c, are the same. From equations (2.17) and (5.20), we see that this requires

$$V'(r_b) = \pm V'(r_c), \tag{5.21}$$

where we choose the minus sign to ensure that there are no other roots between the two horizons. This condition, along with that $V(r)$ has roots at r_b and r_c, implies that $V(r)$ takes the form[17]

$$V(r) = 1 - \frac{2r_b r_c}{(r_b + r_c)\, r} + \frac{r_b^2 r_c^2}{(r_b + r_c)^2\, r^2} - \frac{r^2}{(r_b + r_c)^2}. \tag{5.22}$$

Comparing this to equation (5.19) we can identify

$$m = \frac{r_b r_c}{r_b + r_c}, \qquad e^2 = \frac{r_b^2 r_c^2}{(r_b + r_c)^2}, \qquad \lambda = \frac{3}{(r_b + r_c)^2}, \tag{5.23}$$

so we see that the condition that the two horizons are of the same temperature forces the charge and the mass of the black hole to be equal,

since $m^2 = e^2$. As mentioned previously, a proper definition of an extremal black hole is that it has zero surface gravity, as is clear from equation (2.17). Due to this, it is not correct to call this black hole extremal, since even though its mass and charge are the same its surface gravity is non-zero.

From these calculations, we can use equations (2.17), (5.20) and (5.22) to calculate the temperature at r_b and r_c in terms of r_b and r_c. As expected, they are the same and take the value

$$T_{r_b} = T_{r_c} = \frac{|r_c - r_b|}{2\pi \left(r_c + r_b\right)^2}. \tag{5.24}$$

This tells us that the black hole and cosmological horizons, r_b and r_c respectively, have the same temperature. A black hole with this property is called lukewarm.

5.3.1 Conformal isometries of the lukewarm black hole

When the black hole is lukewarm, that is when the temperatures of the two horizons are equal, we put $e^2 = m^2$ and $\lambda = 3$ by choosing $r_b + r_c = 1$, so $V(r)$ becomes

$$V(r) = \frac{(r-m)^2 - r^4}{r^2}, \tag{5.25}$$

and the horizons are positioned at the roots of $V(r)$, as usual. We obtain four roots,

$$\begin{aligned} r_0 &= -\frac{1}{2}\left(1 + \sqrt{1+4m}\right), \quad r_a = \frac{1}{2}\left(-1 + \sqrt{1+4m}\right), \\ r_b &= +\frac{1}{2}\left(1 - \sqrt{1-4m}\right), \quad r_c = \frac{1}{2}\left(+1 + \sqrt{1-4m}\right), \end{aligned} \tag{5.26}$$

and as mentioned above, $r_0 < 0 < r_a < r_b < r_c$.

Since the extremal charged black hole with a zero cosmological constant has a conformal isometry that interchanges the event horizon and null infinity, we follow the same line of thinking and define a new coordinate $x' = x'(r)$ that under $x = 1/x'$, will interchange the event horizon at r_b with the cosmological horizon at r_c,

$$x'(2m) = 1, \qquad x'(r_b) = 0, \qquad x'(r_c) = \infty. \tag{5.27}$$

But the formula for Möbius transformations,

$$f(z) = \frac{az+b}{cz+d}, \tag{5.28}$$

where $ab - cd \neq 0$, tells us that

$$x'(r) = \frac{r - r_b}{r_c - r}\frac{r_c}{r_b}. \tag{5.29}$$

We see that this transformation is different from the one Couch and Torrence[14] used. While we could define an almost identical transformation to theirs to get the results that are to follow, we use this one as it simplifies the calculations quite a bit. If we now invert this coordinate

$$x' \to x = 1/x', \tag{5.30}$$

the metric takes the form

$$ds^2 = -V\left(\frac{1}{x}\right)dt^2 + \frac{dx^2}{V\left(\frac{1}{x}\right)}\left(\frac{dr}{dx'}\left(\frac{1}{x}\right)\frac{dx'}{dx}\right)^2 + r^2\left(\frac{1}{x}\right)d\Omega_2^2, \tag{5.31}$$

What we now want to show is that this metric is conformal to the original metric. That is, we want to show that the right hand side of equation (5.31) is equal to

$$\Omega^2(x)\left(-V(x)dt^2 + \frac{dx^2}{V(x)}\left(\frac{dr}{dx}\right)^2 + r^2(x)d\Omega_2^2\right), \tag{5.32}$$

where $\Omega^2(x)$ is some function of x chosen that the two sides are equal. Thus the problem results in solving three equations, one for each of the metric terms, and finding a common $\Omega(x)$. The $\Omega(x)$ that does the trick for the last term is easy to find as x only enters the equation through r. It is

$$\Omega(x) = \frac{xr_b + r_c}{xr_c + r_b}, \tag{5.33}$$

and after some calculations it is easily verified that it also works for the other two terms. In order to visualize these results better, it is helpful to draw a Carter-Penrose diagram of this spacetime.

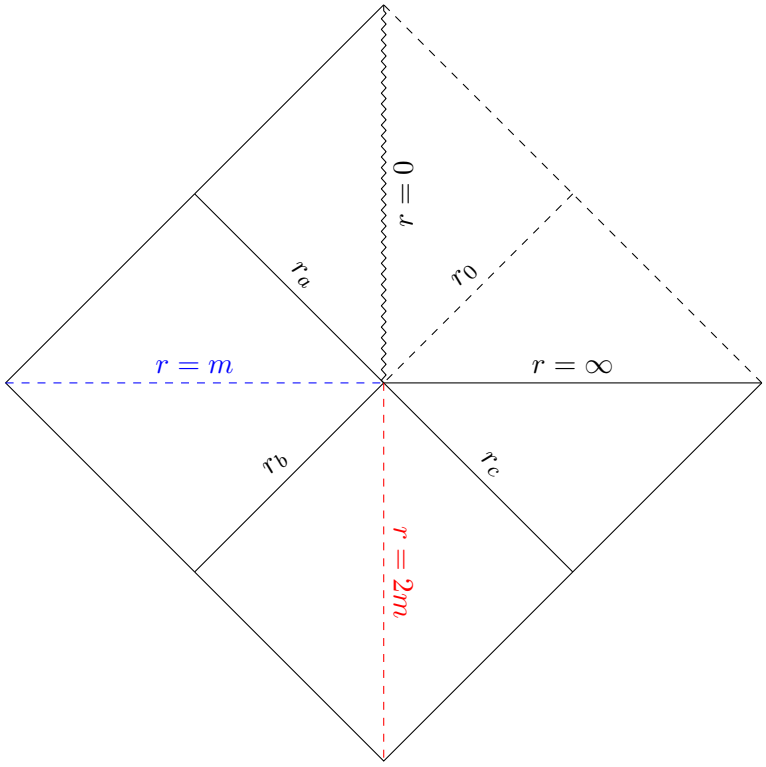

Figure 5.9: Carter-Penrose diagram for the conformally extended Reissner-Nordström de Sitter black hole.

Remember that due to our definition of the coordinate x' in equation (5.29), when it is inverted by defining x, we map $r = 2m$ into itself and r_b into r_c and vice versa. We notice that $x' = 1$, corresponding to $r = 2m$, is not the only fixed point of the transformation, $x = -1$ is also mapped into itself and corresponds to $r = 0$. If looked at from the point of figure 5.9, we can speculate that the coordinate transformation from equation (5.30) maps the areas to the left and right of the surface $r = 2m$ into each other. This leads to the question whether the conformal isometry is extended beyond r_b and r_c. An easy calculation shows that

$$x'(m) = \frac{r_c - 1}{r_c}, \qquad x'(\infty) = \frac{r_c}{r_c - 1}, \tag{5.34}$$

in other words, the surface $r = m$ is conformal to the surface $r = \infty$, which is flat so the former surface is conformally flat. This can also be seen from appendix A. But there is no reason to stop here. It turns out that the unphysical root, r_0, maps into the inner black hole root, r_a, under these transformation just as r_b and r_c do. That is

$$x'(r_0)x'(r_a) = 1, \tag{5.35}$$

And as was mentioned above, since both $r = 2m$ and $r = 0$ are fixed points of this transformation, we see that this transformation acts not only as as a mirroring of the regions on either side of $r = 2m$ but $r = 0$ as well. This goes back to what was discussed in chapter 2 about the physical spacetime M being contained in the unphysical spacetime $\hat{M}$. Here, the unphysical root r_0, which lies in a region of the unphysical spacetime $\hat{M}$ that is not in the physical spacetime M, is conformal to the physical root r_a, which is a part of the physical spacetime M. As was mentioned above, when choosing the first transformation defined by equation (5.27) we could have mapped different points into each other to achieve the same results. Figure 5.9 tells us which points we could have chosen as any of the three pairs (r_b,r_c), (r_0,r_a) or (m,∞) along with either $r = 2m$ or $r = 0$ mapped into itself would have achieved the same results.

Since the region between $r = m$ and $r = 0$ are to be mapped into negative values of r beyond $r = \infty$ this solution shows a formal analogy between certain systems in statistical physics where negative temperatures show up when going beyond infinity. That is, going further than positive infinity brings you to negative infinity and eventually you approach zero from below. Or in other words, $r_0 < 0$ does not lie below r_a as expected but rather above infinity.

While this similarity is interesting and certainly a part of the complete solution, it is doubtful that it holds any physical meaning. However, in certain approaches to numerical relativity it has been suggested that instead of looking at the physical spacetime one should focus on the extended spacetime[18]. In what we have shown, we see that in some cases, the extended spacetime can contain singularities. In particular, we see that the extended spacetime of equation (5.12) contains a timelike singularity passing through spatial infinity. This suggests that what we have shown here could be of some importance in numerical relativity even though it probably holds no physical meaning.

This discussion might be worth keeping in mind when considering Friedrich's[19] program since in both the conformal isometry discussed in this section and the conformal isometry of the extremal Reissner-Nordström black hole as discussed by Couch and Torrence, a singularity in the unphysical spacetime passes through spatial infinity, i^0 which might influence numerical calculations there.

Chapter 6

Kerr - a spinning black hole

We turn now to the spinning black hole without charge. While it would be possible to consider a spinning black hole with charge we do not do this as it does not change things in any very interesting way and simply complicates some formulas. Many of the methods used in chapter 5 will not work here as the spacetime is not spherically symmetric. A spinning black hole is described by the Kerr metric[20],

$$\begin{aligned} ds^2 = &-\left(1-\frac{2mr}{r^2+a^2\cos^2\theta}\right)\left(dv+a\sin^2\theta d\phi\right)^2 \\ &+2\left(dv+a\sin^2\theta d\phi\right)\left(dr+a\sin^2\theta d\phi\right) \\ &+\left(r^2+a^2\cos^2\theta\right)\left(d\theta^2+\sin^2\theta d\phi^2\right), \end{aligned} \tag{6.1}$$

where a is the angular momentum per unit mass. We notice that this metric is more complicated than the metric for the charged black hole due to the off diagonal terms. This is not where the difference ends but we will postpone that discussion until we switch coordinates.

There are some things we can observe about the spacetime before changing to a more suitable coordinate system. We notice that the metric has a problem when when $r^2+a^2\cos^2\theta=0$, that is when

$$r=0, \qquad\qquad \theta=\frac{\pi}{2},\frac{3\pi}{2}. \tag{6.2}$$

This turns out to be an actual curvature singularity. This singularity is often called a ring singularity as it it forms a circle if you consider that the singularity happens at any value of ϕ but for a fixed value of r and θ. From the metric itself, we see immediately that there are two Killing vectors,

$$\xi^a=(\partial_v)^a\,, \qquad\qquad \psi^a=(\partial_\phi)^a\,, \tag{6.3}$$

which correspond to time and axial symmetry, respectively.

It can be shown that the general form of a Killing vector field for this spacetime is a linear combination of these two. That is, the isometry group is two dimensional, as opposed to both the Schwarzschild and Reissner-Nordström spacetimes which have a four dimensional isometry group.

Letting a go to zero puts the metric in the form

$$ds^2 = -\left(1 - \frac{2m}{r}\right) dv^2 + 2dvdr + r^2\left(d\theta^2 + \sin^2\theta d\phi^2\right), \tag{6.4}$$

which is the Schwarzschild metric in advanced Eddington-Finkelstein coordinates, defined analogously to the coordinates in equation (5.13) with $e = 0$.

Now, let us switch to coordinates better suited for some calculations. Defining t and then $\tilde{t}$ and $\tilde{\phi}$ by

$$\begin{aligned} v = t + r, \qquad t &= \tilde{t} + 2m \int \frac{rdr}{r^2 - 2mr + a^2}, \\ \phi &= -\tilde{\phi} - a \int \frac{dr}{r^2 - 2mr + a^2}, \end{aligned} \tag{6.5}$$

puts the metric into the so called Boyer-Lindquist form

$$ds^2 = -e^{2\nu}d\tilde{t}^2 + \frac{\rho^2}{\Delta}dr^2 + \rho^2 d\theta^2 + \frac{\Delta \sin^2\theta}{e^{2\nu}}\left(d\tilde{\phi} - \Omega d\tilde{t}\right)^2, \tag{6.6}$$

where

$$\begin{aligned} \rho^2 = r^2 + a^2\cos^2\theta, \qquad & \Delta = r^2 - 2mr + a^2, \\ e^{2\nu} = \frac{\Delta\rho^2}{A}, \qquad & \Omega = \frac{2amr}{A}, \\ A = \left(r^2 + a^2\right)^2 - a^2\Delta\sin^2\theta. & \end{aligned} \tag{6.7}$$

Since the form of transformation from $\tilde{t}$ to v is the same as the one covered in chapter 2 the Killing vectors from equation (6.3) are unchanged except that $\tilde{t}$ replaces v and $\tilde{\phi}$ replaces ϕ.

Let us discuss briefly an important difference between the spinning black hole and the other types of black holes we know. Both the Schwarzschild and Reissner-Nordström metrics can be naturally split into space and time parts. This can be seen from the fact that their Killing vector fields are hypersurface forming. Whether any of the Killing vector fields of the Kerr spacetime are hypersurface forming can be checked with Fröbenius'

theorem[4], which states that a vector field t^a is hypersurface forming if and only if

$$t_{[a}\nabla_b t_{c]} = 0. \tag{6.8}$$

A short calculation confirms that this does not hold for $t^a = \partial_t^a$,∂_ϕ^a or a linear combination of those two so none of the Killing vectors of the Kerr metric are hypersurface forming. Whether a vector field is hypersurface forming or not can be visualized in the following way. Consider a tangent three-plane to a vector field and if these three-planes form a hypersurface throughout the spacetime, the vector field is said to be hypersurface forming. This means that the Kerr spacetime does not split naturally into space and time parts and visualizing it completely is much harder as one can not suppress any of the four dimensions.

We notice that in addition to the singularity defined by (6.2) there are coordinate singularities at the roots of $\Delta = 0$. These are the two horizons of the black hole and they are positioned at $\Delta = 0$ which has roots at

$$r_\pm = m \pm \sqrt{m^2 - a^2}, \tag{6.9}$$

which has the exact same form as the horizons of the charged black hole with e replacing a. This means that the discussion there about $r_\pm$ becoming imaginary also holds here so we look only at $a^2 \leq m^2$. This also tells us that, just as for the charged black hole, the black hole is extremal when $a^2 = m^2$ and there is only one horizon sitting at $r = m$ in that case. That is, a black hole with $a^2 = m^2$ has the maximum available angular momentum while remaining a black hole. Just as for the charged black hole, these two roots split the spacetime into three regions or blocks, depicted in a Carter-Penrose diagram drawn for the equatorial plane in figure 6.1. Region I which is outside the black hole, region II which is between the two horizons of the black hole and region III which is inside the inner horizon and contains the curvature singularity. Region III is significantly different from region III in the Reissner-Nordström spacetime in the sense that it provides an extra asymptotic region when $r \to -\infty$. As opposed to the Einstein-Rosen bridge of the Schwarzschild solution, whose $t = 0$ hypersurface is symmetric around the event horizon, the three regions of Kerr are not symmetric as the spacetime behaves differently at $r \to \infty$ and $r \to -\infty$. In fact, it behaves as Schwarzschild when $r \to \infty$ but Schwarzschild with negative mass at infinity when $r \to -\infty$, which is sort of a sick spacetime as it has a naked singularity. Along with this, the fact that

$$\left\|\partial_\phi^a\right\|^2 \propto A$$

can become negative when $r < 0$ in region III means that closed timelike curves exist there.

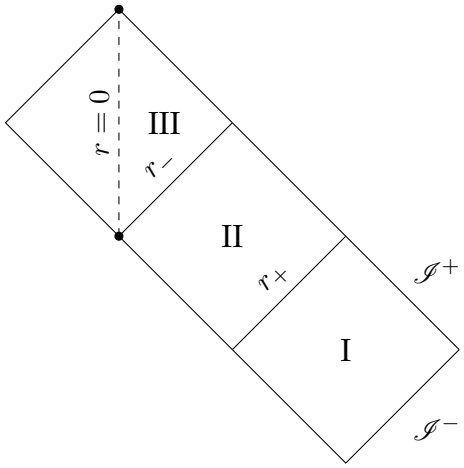

Figure 6.1: The Carter-Penrose diagram of the equatorial plane of the Kerr spacetime. Here each point in the picture represents a circle.

If we look at the norm of the timelike Killing vector field, $\|\xi^a\|$, we see that it is spacelike in a region outside the event horizon. That is, we see that it is null when

$$0 = r^2 + a^2 \cos^2\theta - 2mr, \tag{6.10}$$

which tells us that

$$r_e = m + \sqrt{m^2 - a^2 \cos^2\theta}. \tag{6.11}$$

Therefore, between r_+ and r_e the timelike Killing vector field is spacelike. This region is called the ergosphere. An observer in the ergosphere can not remain stationary since he would have to travel faster than the speed of light to follow the orbits of ξ^a. In figure 6.2 we draw a throat picture of the Kerr spacetime. This shows the region where ξ^a is spacelike colored red and the ergosphere as the part of that region above the curve indicating r_+. The reason for drawing a diagram like this instead of a typical polar plot is clear when we notice that the curvature singularity defined by equation (6.2) is represented as a pair of points on the curve $r = 0$, corresponding to $\theta = \pi/2{,}3\pi/2$, while on a polar plot the point $r = 0$ would include all values of θ.

Due to this behaviour we see that the coordinates in the Kerr spacetime behave differently than in the Reissner-Nordström spacetime. For the

Reissner-Nordström case, both g_{rr} and g_{tt} changed signs at the horizons and became time- and spacelike, respectively, between r_+ and r_-. But for the spinning case, we see that this does not happen. Both of them still change sign but it does not happen at the same place. This happens due to the spacetime not being spherically symmetric and is the reason why our method for drawing Carter-Penrose diagrams can only draw the diagram for a fixed θ as we did in figure 6.1.

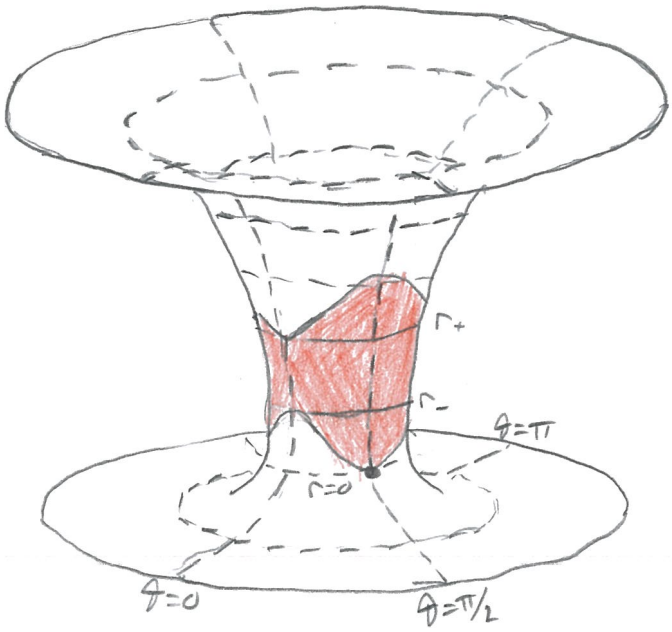

Figure 6.2: The throat picture of the Kerr spacetime which shows a surface where both t and ϕ are kept fixed. We see that all three blocks are present lying in their respective places according to $r = 0$, $r = r_+$ and $r = r_-$. We also see very clearly that the ring singularity is only visible as two points at $r = 0$, for $\theta = \pi/2$ and $3\pi/2$. The region where the timelike Killing vector field is spacelike is colored in red. This figure is and the throat pictures that follow are all inspired by Carter[21].

As was the case for the charged black hole, it is of interest to see what happens to region II when the black hole is extremal. As region II is defined as the region between the two horizons, $r_\pm$, given by equation (6.9), we see that in the scaling limit they take the same value. This leads us to believe that the region might have vanished. However, we can write down an equation similar to (5.4) for a timelike curve at constant t and ϕ going between r_- and r_+

$$L = -\int_{r_+}^{r_-} dr \sqrt{\frac{r^2 + a^2\cos^2\theta}{(r_+ - r)(r - r_-)}}, \tag{6.12}$$

which is plotted as a function of a and θ in figure 6.3.

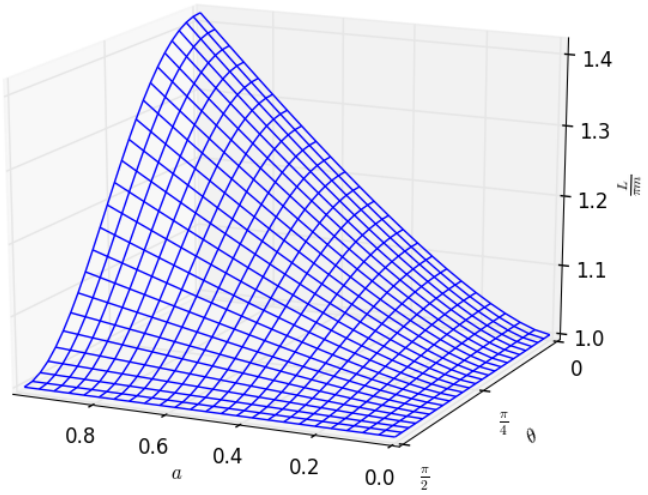

Figure 6.3: The scaled distance between r_+ and r_-, $L/\pi m$, as a function of a and θ

We see that the edges on the graph, $a = 0$ or $\theta = \pi/2$, are where the minimum value for $L/(\pi m)$, unity, occurs and we see that it is always at least that large and always larger than zero, as was the case for the charged black hole. Just as for the charged black hole, this calculation suggests that the region between r_+ and r_- vanishes. But, we do not take it literally and only use it to serve as a warning that taking limits must be done with care.

6.1 Near-horizon limit

Just as for the charged black hole we can look at the geometry close to the horizon of the extremal spinning black hole[22]. To this end, we define new coordinates

$$r = m + \varepsilon x, \qquad \tilde{t} = 2m^2 \frac{t}{\varepsilon}, \qquad \tilde{\phi} = \phi + a\frac{t}{\varepsilon}, \tag{6.13}$$

where $x > 0$ and as before, ε is a dimensionless parameter that goes to zero as we zoom in on the horizon. Doing this coordinate transformation and letting $\varepsilon \to 0$ gives the metric

$$ds^2 = m^2\left(1+\cos^2\theta\right)\left(-x^2dt^2 + \frac{dx^2}{x^2} + d\theta^2\right) + \frac{4m^2\sin^2\theta}{1+\cos^2\theta}\left(d\phi + xdt\right)^2, \tag{6.14}$$

which, as we will see below, is conformal to the product of squashed three-dimensional anti-de Sitter space with a circle as given by equation (3.14). We see that the squashing factor is θ-dependent and given by

$$\alpha = \frac{2\sin\theta}{1+\cos^2\theta}. \tag{6.15}$$

This case is slightly different as the squashing or stretching now depends on where you are on the circle but for each θ it is still the usual squashing or stretching. Equation (6.15) tells us a few things about the squashing. As mentioned above the squashing or stretching is θ dependent. When $\alpha < 1$ the spacetime is squashed while it is stretched if $\alpha > 1$. At the poles $\alpha = 0$ and we see that the metric reduces to a form of adS_2 as given by equation (5.7) but as the ϕ part of the metric disappears when we squash completely it is only $adS_2 \times S^1$, not $adS_2 \times S^2$. As was mentioned in section 3.1 we see that when $\alpha = 1$ the metric takes the form of $adS_3 \times S^1$. In other words, when

$$2\sin\theta = 1 + \cos^2\theta, \tag{6.16}$$

which happens at

$$\sin\theta_S = \sqrt{3} - 1, \tag{6.17}$$

so from the previous discussion we see that between $\theta = 0$ and θ_S, the spacetime is squashed while from θ_S and to $\theta = \pi/2$ it is stretched. We

will see later that this particular value of θ is also of importance when it comes to the Killing vectors of the metric but first we will look at other things. Notice that due to this squashing the isometry group reduces to $SL(2,\mathbb{R}) \times U(1)$ instead of $SL(2,\mathbb{R}) \times \mathbb{R}$ as was the case in section 3.1 due to ϕ being periodic.

For completeness, we can analytically extend the spacetime by following what Bardeen and Horowitz showed in [22] so that it becomes geodesically complete with a coordinate transformation

$$x = \cosh\omega \cos\tau + \sinh\omega, \quad t = \frac{\cosh\omega \sin\tau}{x}, \quad \phi = \sigma + f(\tau,\omega), \tag{6.18}$$

where $f(\tau,\omega)$ is chosen such that the metric simplifies. In these coordinates the metric takes the form

$$ds^2 = m^2\left(1+\cos^2\theta\right)\left(-\cosh^2\omega d\tau^2 + d\omega^2 + d\theta^2\right) + \frac{4m^2\sin^2\theta}{1+\cos^2\theta}\left(d\sigma + \sinh d\tau\right)^2. \tag{6.19}$$

In these coordinates, it is obvious that it is indeed squashed adS_3, given by equation (3.14), with a θ dependent squashing parameter. If the coordinates are allowed to run over their full ranges, and not the one restricted from the transformation (6.18), this metric covers all of squashed adS_3 .

Just as for the near-horizon geometry of the charged black hole, the spacetime described by the metric (6.14) does not cover all of squashed $adS_3 \times S^1$. However, rather than going through the whole procedure of seeing what restrictions apply when going from our metric to the embedding space, we see that the adS_2 part of the metric (6.14) is identical to the adS_2 part of the near-horizon metric for the charged black hole, equation (5.7). Since there are no restrictions on any of the other coordinates, we see that the region covered by the metric (6.14) of all squashed adS_3 is simply the region of adS_2 shown in figure 5.3 times S^1 and something extra from the last part of the metric.

6.2 $a \to m$ scaling limit

In chapter 5 we addressed what happens to region II using an alternative limit first studied by Carroll et al, but made their observation more nearly global, by covering all three regions using Eddington-Finkelstein coordinates. Now we want to see if the same procedure can be applied to Kerr. Following what we did for the charged black hole, we look at the scaling limit of the spinning black hole. Even though we did write the Kerr metric down in a form which is analogous to Eddington-Finkelstein

coordinates in equation (6.1) we will define the new coordinates in a slightly different, but equivalent, way

$$dv = d\tilde{t} + \left(r^2 + a^2\right)\frac{dr}{\Delta}, \qquad d\phi' = d\tilde{\phi} + a\frac{dr}{\Delta}, \tag{6.20}$$

which puts our metric, (6.6), into the form

$$\begin{aligned} ds^2 = &-e^{2\nu}dv^2 + 2dvdr + \rho^2 d\theta^2 - 2a\sin^2\theta dr d\phi' \\ &+ \frac{\Delta\sin^2\theta}{e^{2\nu}}\left(d\phi' - \Omega dv\right)^2. \end{aligned} \tag{6.21}$$

Now we are ready to take the scaling limit. Defining new coordinates by

$$r = m + \varepsilon\chi, \qquad v = \left(m^2 + a^2\right)\frac{\psi}{\varepsilon}, \qquad \phi' = \phi + \frac{a\psi}{\varepsilon}, \tag{6.22}$$

where ε now stands for $\sqrt{m^2 - a^2}$ and not a dimensionless parameter. Performing this transformation and taking the limit $\varepsilon \to 0$ we obtain

$$\begin{aligned} ds^2 = &\, m^2\left(1 + \cos^2\theta\right)\left(-\left(\chi^2 - 1\right)d\psi^2 + 2d\psi d\chi + d\theta^2\right) \\ &+ \frac{4m^2\sin^2\theta}{1 + \cos^2\theta}\left(d\phi + \chi d\psi\right)^2, \end{aligned} \tag{6.23}$$

which is squashed or stretched $adS_3 \times S^1$ just as for the near-horizon limit. We notice that the squashing factor is still given by equation (6.15).

As usual, the region covered by the metric (6.23) does not cover the whole spacetime. However, the same logic applies here as in the near-horizon case above. That is, the region which our metric (6.23) covers of squashed adS_3 simply the three regions depicted in figure 5.6 times S^1 and the same extra piece as in the near-horizon case.

6.3 Killing vector fields

A useful concept when discussing Killing vector fields is a so-called bivector. In geometric terms, a bivector generalizes the idea of a vector in the sense that while a vector can be thought of as a directed line segment a bivector can be thought of as an oriented plane segment. In three dimensions, given two vectors $\mathbf{a}$ and $\mathbf{b}$ their exterior product $\mathbf{a} \wedge \mathbf{b}$ is a bivector. For this particular bivector, its magnitude is the area of the parallelogram formed by $\mathbf{a}$ and $\mathbf{a}$. Its orientation is that of a rotation that would make $\mathbf{a}$ parallel to $\mathbf{b}$. Note that this bivector is antisymmetric.

This idea can be extended to Killing vectors and Killing bivectors. A Killing bivector of the Kerr metric is a rank two antisymmetric tensor

$$K^{ab} = 2\xi^{[a}\psi^{b]}. \tag{6.24}$$

Note that K^{ab} is left unchanged by transformations of the form

$$\begin{aligned} \xi^a = \partial_t^a &\to \partial_t^a + c\partial_\phi^a, \\ \psi^a = \partial_\phi^a &\to \partial_\phi^a + c\partial_t^a, \end{aligned} \tag{6.25}$$

as is easily verified. By considering a two-plane in tangent space, characterized by the Killing bivector K_{ab} and spanned by the two Killing vectors in equation (6.3), we can make a statement about the existence of a Killing vector in the spacetime. That is, if

$$\frac{1}{2}K_{ab}K^{ab} \tag{6.26}$$

is negative, the two-plane characterized by the Killing bivector is timelike and therefore a Killing vector must exist. For the metric given by equation (6.6) we see that

$$\begin{aligned} \frac{1}{2}K_{ab}K^{ab} &= \partial_{\tilde{t}a}\partial_{\tilde{\phi}b}\left(\partial_{\tilde{t}}^a\partial_{\tilde{\phi}}^b - \partial_{\tilde{t}}^b\partial_{\tilde{\phi}}^a\right) \\ &= \|\partial_{\tilde{t}}\|^2 \left\|\partial_{\tilde{\phi}}\right\|^2 - \left(\partial_{\tilde{t}} \cdot \partial_{\tilde{\phi}}\right)^2 \\ &= g_{\tilde{t}\tilde{t}}g_{\tilde{\phi}\tilde{\phi}} - g_{\tilde{t}\tilde{\phi}}^2 \\ &= -\sin^2\theta\Delta. \end{aligned} \tag{6.27}$$

Since Δ is positive everywhere outside the horizon we can say that there exists a timelike Killing vector everywhere outside the horizon. Since the idea of a bivector is that of two-planes we can ask whether a bivector is

surface forming, just as we did for the tangent two-planes of Killing vector fields. As Carter points out[23], the condition for the Killing bivector K_{ab} to be surface forming is

$$\begin{aligned} \xi_{[a;b}K_{cd]} &= 0 \\ \psi_{[a;b}K_{cd]} &= 0, \end{aligned} \tag{6.28}$$

which can be seen to vanish due to the fact that the metric only depends on r and θ and the fact that the Killing bivector is antisymmetric. Therefore the Killing bivector is actually surface forming for the Kerr spacetime in Boyer-Lindquist coordinates. However, this is not surprising since if one considers how these coordinates were defined, it is clear that this property was used to define them.

In the near-horizon coordinates defined by (6.13) one of the Killing vector fields lies along ∂_t since

$$\begin{aligned} \partial_t &= \frac{\partial \tilde{t}}{\partial t}\partial_{\tilde{t}} + \frac{\partial \tilde{\phi}}{\partial t}\partial_{\tilde{\phi}} \\ &= \frac{1}{\lambda}\left(2m^2\partial_{\tilde{t}} + a\partial_{\tilde{\phi}}\right) \end{aligned}$$

which is a linear combination of the two Killing vectors from equations (6.3) in the Boyer-Lindquist coordinates. Therefore

$$\chi^a \propto (\partial_t)^a \,.$$

Since the coefficients in front of $\partial_{\tilde{t}}$ and $\partial_{\tilde{\phi}}$ can be scaled arbitrarily we choose the most general Killing vector field to be

$$\chi^a = (\partial_{\tilde{t}})^a + \Omega_H \left(\partial_{\tilde{\phi}}\right)^a, \tag{6.29}$$

where $\Omega_H = \frac{a}{2mr_+} = \frac{1}{2m}$ is the angular velocity of the horizon in the extremal case. This constant is chosen such that χ^a is null along the horizon. We can see this if we look at one of the principal null vectors[4] of the metric at the horizon $\Delta = 0$,

$$\begin{aligned} \ell^a &= \frac{1}{\Delta}\left(\left(r^2+a^2\right)(\partial_{\tilde{t}})^a + a(\partial_{\tilde{\phi}})^a + \Delta(\partial_r)^a\right), \\ \left.\frac{\Delta\ell^a}{r^2+a^2}\right|_{\Delta=0} &= (\partial_{\tilde{t}})^a + \frac{a}{r^2+a^2}(\partial_{\tilde{\phi}})^a + \left.\frac{\Delta}{r^2+a^2}(\partial_r)^a\right|_{\Delta=0}, \\ 0 &= (\partial_{\tilde{t}})^a + \frac{a}{\left(r_+^2+a^2\right)}(\partial_{\tilde{\phi}})^a \\ &= (\partial_{\tilde{t}})^a + \frac{a}{2mr_+}(\partial_{\tilde{\phi}})^a, \end{aligned}$$

where $r_+ = a = m$ in the extremal case. We can also check whether this Killing vector field is null anywhere else in the near-horizon geometry,

$$\begin{aligned} 0 &= \chi^a \chi_a \\ &= -m^2 x^2 \left(1 + \cos^2\theta\right) \left(1 - \frac{4\sin^2\theta}{\left(1+\cos^2\theta\right)^2}\right), \end{aligned} \tag{6.30}$$

which we recognize to be the same position as that of where the near horizon metric is adS_3, θ_S. This means that there are two surfaces where the Killing vector field has zero length, the Killing horizon and the surface defined by the above θ value which is timelike. We see that this Killing vector field is timelike when we squash ($\alpha^2 < 1$) and spacelike when we stretch ($\alpha^2 > 1$) as long as we are not at the Killing horizon.

Let us do the same calculation for the original metric given by equation (6.6). That is, let us look at the norm of the Killing vector field

$$\begin{aligned} \|\chi^a\|^2 &= \left\| \partial_{\tilde{t}} + \frac{a}{2mr_+} \partial_{\tilde{\phi}} \right\|^2 \\ &= g_{\tilde{t}\tilde{t}} + \frac{a}{mr_+} g_{\tilde{t}\tilde{\phi}} + \left(\frac{a}{2mr_+}\right)^2 g_{\tilde{\phi}\tilde{\phi}} \\ &= -\frac{r - r_+}{4m^2 r_+^2 \rho^2} f(r,\theta). \end{aligned} \tag{6.31}$$

where

$$f(r,\theta) = \left(4m^2 r_+^2 \left(r - r_-\right) - a^2 \sin^2\theta \left(4m^2 \left(r - r_+\right) + \left(r - r_-\right)\left(\rho^2 + 2mr\right)\right)\right). \tag{6.32}$$

As expected, the Killing vector field goes null at the event horizon however it does also go null when $f(r,\theta) = 0$. The surface defined by $f(r,\theta) = 0$ is called the velocity of light surface[24]. What this means is that a timelike observer inside the velocity of light surface can corotate with the black hole[25]. When a is very small, the surface moves to infinity and when $\left(\frac{a}{m}\right)^2 = 2\left(\sqrt{2} - 1\right)$ the surface coincides with the ergosphere at $\theta = \pi/2$, as can be seen from putting $\theta = \pi/2$ in equations (6.32) and (6.11) to find that $r = 2m$ at the equator for the ergosphere. Solving for a/m, we see that the velocity of light surface moves closer and closer to the black hole with increasing a/m. We draw the case when the velocity of light surface and the ergosphere meet at $\theta = \pi/2$ in figure 6.4.

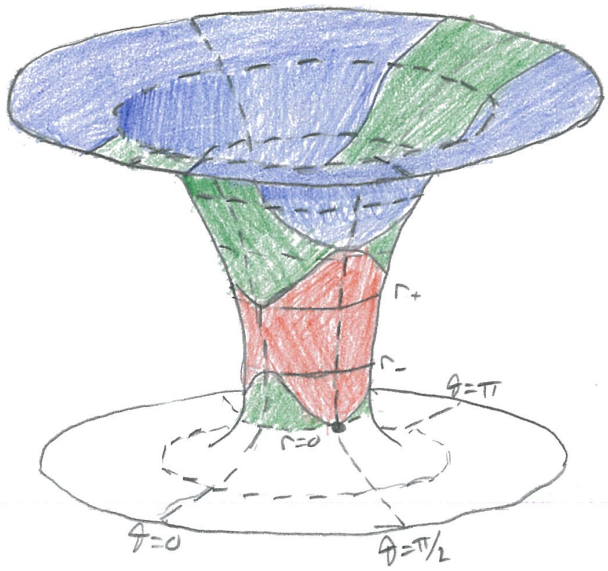

Figure 6.4: A throat diagram, a surface with both t and ϕ kept fixed as before, of the velocity of light surface (as the boundary between the blue and green regions) drawn for the value $(a/m)^2 = 2(\sqrt{2}-1)$ when it coincides with the ergosphere at $\theta = \pi/2$. Just as in figure 6.2 the three regions are visible and the ring singularity shows up as two points. The blue region is where the Killing vector field is spacelike and green and red where it is timelike.

This figure tells us that a timelike observer can only corotate with the black hole if he is in the green or red regions. As mentioned above, the surface approaches the horizon as $a/m \to 1$ but as is usually the case when considering the scaling limit, that is not the whole story.

Let us therefore consider now what happens in the extremal case and not just when approaching it. When $a^2 = m^2$, equation (6.31) becomes

$$\|\chi^a\|^2 = -\frac{(r-m)^2}{4m^4\rho^2} f'(r,\theta), \tag{6.33}$$

where

$$f'(r,\theta) = \left(4m^4 - m^2\sin^2\theta\left(4m^2+\rho^2+2mr\right)\right), \tag{6.34}$$

which goes null at θ_S, defined by equation (6.17). This was to be expected as the near-horizon limit zoomed in on the horizon and we saw that the Killing vector field went null at this particular θ value. However, we also

notice that before the black hole becomes extremal you can always find a region arbitrarily close to the horizon where the Killing vector field is timelike. But once the black hole is extremal, the surface where the Killing vector field is null crosses the horizon and at certain points outside the horizon, the Killing vector field is always spacelike. Solving $f'(r,\theta) = 0$ outside the horizon gives the exact curve at which the Killing vector field goes null

$$\frac{r}{m} = \frac{1}{\sin\theta}\left(2 - \sin^2\theta\right) - 1, \tag{6.35}$$

which we can use to schematically draw the different regions where the Killing vector field goes time-, spacelike or null in a throat diagram. We see that $r \to \infty$ as $\theta \to 0$ and that $r = 0$ when $\theta = \pi/2$ which is at the curvature singularity. Using these two points along with the fact that we know that $\sin\theta = \sqrt{3} - 1$ when $r = m$ we can draw figure 6.5.

This means that for the extremal spinning black hole, it is not possible to corotate with the black hole except in a small r dependent region around the azimuthal axis. This region is drawn in green in figure 6.5

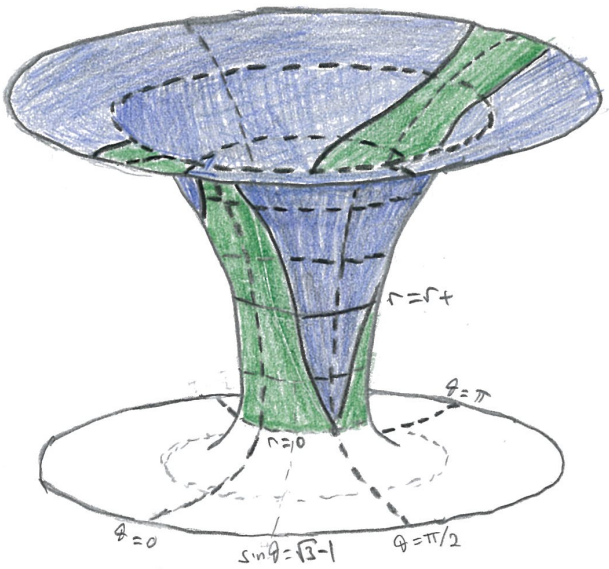

Figure 6.5: The extremal Kerr throat, as usual drawn as a surface where both t and ϕ are kept fixed. Since it is extremal, we see that there is only one horizon sitting at $r = r_+ = m$ and therefore there are only two regions visible, regions I and III. The ring singularity remains as two points at $r = 0$. The blue region is roughly where the Killing vector field of equation (6.29) is spacelike and the green region where it is timelike.

These results might seem to contradict what was said above about the existence of a timelike Killing vector everywhere outside the horizon. That is, first we showed that there exists a timelike Killing vector everywhere outside the horizon. These results held for both non-extremal and extremal black hole as Δ is positive outside the horizon in both cases. After that we showed that for the extremal black hole the most general Killing vector field is spacelike everywhere in a certain region on both sides of the horizon of the black hole. However, this is not a contradiction to the previous statement even though it seems to be at first sight.

The answer lies in the difference between a Killing vector and a Killing vector field. In the first calculation, we showed that there exists a timelike *killing vector* while in the second calculation we showed that a *Killing vector field* is spacelike in a certain region around the horizon.

When one makes this distinction there is no contradiction as one could think of a combination, not linear, of Killing vectors that do not form a Killing vector field, for example if the coefficients in the combination would depend on the coordinates. This would mean that there exists a timelike

Killing vector everywhere outside the horizon but we can not make a statement about a timelike Killing vector field, but it probably does not exist.

Chapter 7

Conclusions

Let us summarize what we have done in this thesis. In preparation for what was to come we reviewed properties of Killing vectors, conformal spacetimes, conformal isometries and anti-de Sitter space and then these things were used to draw the Penrose diagrams of various spacetimes. In particular, along with Penrose diagrams for Minkowski space and anti-de Sitter space an algorithm was put forth on how to draw the Penrose diagrams of spherically symmetric spacetimes.

After that the charged black hole, described by the Reissner-Nordström metric, was discussed. The near-horizon and $e \to m$ scaling limits were taken and the resulting spacetimes investigated. By using coordinates that cover all three blocks of the metric, we were able to clarify a puzzling result due to Carroll et al[13] and arrive at a more nearly global result.

Next the charged black hole was put in a positively curved cosmological background and just as for the extremal charged black hole, it was shown to possess a conformal isometry just as Brännlund pointed out[15]. The new contribution here is that this isometry was extended throughout the complete spacetime. In fact, the isometry is extended even further as the unphysical root of the Reissner-Nordström de Sitter metric is conformal to one of the physical roots. While it is doubtful that this has any physical meaning it might hold a lesson for one approach to numerical relativity.

A discussion of the Kerr black hole went along the same lines as for the charged black hole. The two limits were discussed and in addition, the behaviour of a horizon Killing vector field was discussed when the black hole became extremal. Similar results had been derived by Amsel et al[25] but using less global coordinates.

As was know from previous work by Amsel et al[25], it turns out that the so-called velocity of light surface, a surface beyond which an observer can no longer corotate with the black hole, makes a discontinuous jump from being completely outside the horizon to being partly inside and partly outside once the black hole is extremal[24]. The velocity of light surface

is of some importance when discussing quantum field theory close to the horizon as in order to define positive and negative energy states, a timelike Killing vector must be available. We provide additional detail to this discussion.

While working on this thesis, new ideas and problems have emerged. A natural follow up to the discussion in chapter 5 on region II of figure 5.1 is to what extent the question about what happens to the region in the limit can be made precise. That is, does it make sense at all to worry about whether it has vanished or not. While it was discussed there, it could be investigated even further in the fashion Geroch suggests the limit $e \to 0$ could be looked at[2]. That is, considering which points lying in the region r_- and r_+ survive in the limit and which do not when the charge vanishes. We believe that Geroch's treatment could be made more precise in order to understand the limiting behavior of the black hole. An idea is that the points between r_- and the hypersurface $r = e^2/m$ are the ones that disappear while the points between $r = e^2/m$ and r_+ will survive. This idea comes from the fact that the Weyl tensor vanishes on this hypersurface and plays a role in section 5.3.

We could ask a similar question of the $e \to m$ scaling limit and see which points vanish and which do not once the limit has been taken. The same question applies to the Kerr spacetime with a replacing e.

Following up on the discussion about the Killing vector field defined in equation (6.29), we can ask whether its norm, as given by equation (6.32), factorizes even further. With symbolic and numerical calculations[1], it can be shown that $f(r,\theta)$ has three real roots,

$$f(r,\theta) \sim P^{(3)}(r), \tag{7.1}$$

where $P^{(3)}(r)$ is a third order polynomial in r that has coefficients which are a function of θ. One of the roots of $P^{(3)}(r)$ corresponds to the velocity of light surface that lies outside the horizon. It turns out that the velocity of light surface is the only root outside the event horizon and that one of the other roots is negative. This means that the Killing vector field will change sign again inside the horizon due to the third root which lies somewhere between the two horizons of the black hole. This tells us that corotating with the black hole inside the black hole might not be possible in certain regions close to the curvature singularity. In the extremal case, the

[1] Jan E. Åman, private communication

corresponding equation is (6.34), which is a second order polynomial and has at most two roots,

$$f'(r,\theta) \sim P^{(2)}(r) \tag{7.2}$$

where $P^{(2)}(r)$ is a second order polynomial in r that has coefficients which are a function of θ. We know that one its roots lies both inside and outside the horizon and corresponds to the velocity of light surface. This root can be interpreted in the way that the two positive roots of the non-extremal case, one inside and one outside the horizon, merge to form this single positive root of the extremal case. The second root is negative and therefore not of very much interest.

We end this thesis by quoting Chandrasekhar[26]

> *"In my entire scientific life...the most shattering experience has been the realization that an exact solution of general relativity, discovered by the New Zealand mathematician Roy Kerr, provides the absolutely exact representation of untold numbers of massive black holes that populate the Universe."*

and conclude that it is worthwhile to explore every mathematical detail, no matter how small or peculiar it may seem, of the black hole solutions of general relativity.

Appendix A

The Weyl tensor for the lukewarm black hole

We present here the Weyl tensor for the lukewarm RNdS spacetime as see that it vanishes at $r = m$ and $r = \infty$.

$$
\begin{aligned}
C_{trtr} &= \frac{2\,(m-r)\,m}{r^4}, \\
C_{t\theta t\theta} &= -\frac{m\,(m-r)\left(m^2-r^2-r\right)\left(m+r^2-r\right)}{r^4}, \\
C_{t\phi t\phi} &= \sin^2\theta C_{t\theta t\theta}, \\
C_{r\theta r\theta} &= \frac{(m-r)\,m}{r^2-2mr-r^4+m^2}, \\
C_{r\phi r\phi} &= \sin\theta C_{r\theta r\theta}, \\
C_{\theta\phi\theta\phi} &= 2m\sin^2\theta\,(r-m)
\end{aligned}
$$

Bibliography

[1] K. S. Thorne, The Astrophysical Journal **191**, 507 (1974).

[2] R. Geroch, Comm. Math. Phys. **13**, 180 (1969).

[3] B. Schutz, *A First Course in General Relativity* (Cambridge University Press, 1985).

[4] R. M. Wald, *General Relativity*, First ed. (University Of Chicago Press, 1984).

[5] S. W. Hawking and G. F. R. Ellis, *The Large Scale Structure of Space-Time (Cambridge Monographs on Mathematical Physics)* (Cambridge University Press, 1975).

[6] M. Eisenberg and R. Guy, The American Mathematical Monthly **86**, pp. 571 (1979).

[7] I. Bengtsson and K. Zyczkowski, *Geometry of Quantum States: An introduction to quantum entanglement*, First ed. (Cambridge University Press, 2008).

[8] S. Detournay, D. Orlando, P. M. Petropoulos, and P. Spindel, Journal of High Energy Physics **2005**, 072 (2005).

[9] I. Bengtsson and P. Sandin, Classical and Quantum Gravity **23**, 971 (2006).

[10] R. Penrose, Structure of space-time, in *Battelle Rencontres: 1967 Lectures in Mathematics and Physics*, edited by C. DeWitt and J. Wheeler, pp. 121–235, New York, 1968, W.A. Benjamin.

[11] M. Walker, Journal of Mathematical Physics **11**, 2280 (1970).

[12] G. S. Hall, Classical and Quantum Gravity **17**, 3073 (2000).

[13] S. M. Carroll, M. C. Johnson, and L. Randall, Journal of High Energy Physics **2009**, 109 (2009).

[14] W. Couch and R. Torrence, General Relativity and Gravitation **16**, 789 (1984).

[15] J. Brännlund, General Relativity and Gravitation **36**, 883 (2004).

[16] S. W. Hawking, Phys. Rev. D **18**, 1747 (1978).

[17] L. J. Romans, Nuclear Physics B **383**, 395 (1992).

[18] J. Frauendiener, Living Reviews in Relativity **3** (2000).

[19] H. Friedrich, Einstein's equation and geometric asymptotics, 1998, arXiv:gr-qc/9804009.

[20] R. P. Kerr, Phys. Rev. Lett. **11**, 237 (1963).

[21] B. Carter, General Relativity and Gravitation **41**, 2873 (2009).

[22] J. Bardeen and G. T. Horowitz, Phys. Rev. D **60**, 104030 (1999).

[23] B. Carter, General Relativity and Gravitation **42**, 653 (2010).

[24] I. Rácz, Classical and Quantum Gravity **17**, 4353 (2000).

[25] A. J. Amsel, G. T. Horowitz, D. Marolf, and M. M. Roberts, Journal of High Energy Physics **2009**, 044 (2009).

[26] S. Chandrasekhar, *Truth and Beauty: Aesthetics and Motivations in Science* (University of Chicago Press, 1990).